COMPUTATIONAL STUDY OF HYDROGEN BONDED COMPLEX OF ETHANOL AND WATER USING VARIOUS FUNCTIONALS ON THE BASIS OF DENSITY FUNCTIONAL THEORY

A Dissertation

Submitted to the Dean Office, Institute of Science and Technology Tribhuvan University, Kirtipur in the Partial Fulfillment for the Requirements of Master's Degree of Science in Physics

By

Anil Pudasaini

T.U. Regd. No.: 5-2-37-23-2014

Exam Roll No: PHY 3118/075

December, 2022

Recommendation

It is certified that **Mr. Anil Pudasaini** has carried out the dissertation work entitled " **COMPUTATIONAL STUDY OF HYDROGEN BONDED COMPLEX OF ETHANOL AND WATER USING VARIOUS FUNCTIONALS ON THE BASIS OF DENSITY FUNCTIONAL THEORY** " under my supervision and guidance.

I recommend the dissertation in the partial fulfillment for the requirement of Master's Degree of Science in Physics.

_____
(Supervisor)
Prof. Dr. Rajendra Parajuli
Department of Physics, Amrit Campus
Tribhuvan University
Thamel, Kathmandu, Nepal

Date: .....

Acknowledgements

First and foremost, I would like to give special thanks from the bottom of my heart to my supervisor, Professor Dr. Rajendra Parajuli, Amrit Campus, T.U., for his guidance, advices, valuable comments and suggestions that were pivotal in the successful completion of this thesis work.

I want to express by graditude to Dr. Lok Bahadur Baral, Campus Chief; Mr. Pitamber Shrestha, M.Sc. Coordinator; Professor Dr. Leela Pradhan Joshi, Head of Department; Dr. Manoj Kumar Chaudhary, Mr. Dhurba Sapkota, Mr. Dinesh Kumar Chaudhary, Mr. Devendra Raj Upadhyay, Mr. Roshan Chalise, and the entire Amrit Campus family for their cooperation and support and University Grants Commission for providing grants for Gaussian and GaussView softwares. Support of all the people is unconditional which help to add quality to my work.

I would also like to extend my appreciation and thanks to my seniors Mr. Santosh Adhikari and Mr. Ganesh Prasad Tiwari, both of them affably shared their expertise from their previous work, and my colleague Mr. Dhan Raj Lawati, Mr. Roshan Poudel, Ms. Rupa Khanal and Ms. Reja Thapa and all my friends of Master with whom I had learned many things throughout this thesis work as well as all of my friends who directly or indirectly helped me to complete this thesis report.

I want to thank my parents and other family members, who has always supported me morally as well as economically and for their love and the encouragement that always keeps me motivated.

Anil Pudasaini

Evaluation

We certify that we have read this dissertation and in our opinion it is good in the scope and quality as a dissertation in the partial fulfillment for the requirement of Master's Degree of Science in Physics.

Evaluation Committee:

Prof. Dr. Rajendra Parajuli
(Supervisor)
Department of Physics
Amrit Campus
Thamel, Kathmandu
Nepal

Asst. Prof. Pitamber Shrestha
Co-ordinator (M.Sc. Physics)
Department of Physics
Amrit Campus
Thamel, Kathmandu
Nepal

Prof. Dr. Leela Pradhan Joshi
(Head)
Department of Physics
Amrit Campus, Tribhuvan University
Thamel,Kathmandu
Nepal

Internal Examiner

External Examiner

Date.:.....

Abstract

Computational study of hydrogen bonded complex of ethanol and water using various functionals on the basis of density functional theory has been carried out using 6-311++G(d,p), 6-311++G(2d,2p), and aug-cc-pVTZ basis sets. We have calculated binding energy, zero point vibrational energy, distance of the bond formed in the complex, bond angle after complex formation, frequency shift, electron density, and laplacian of electron density for the ethanol and water complex. The binding energy of the complex was found to be in the range of -4.258 kcal/mole to -6.232 kcal/mole . We have calculated the zero-point vibrational energy of the complex and found to be in the range of 1.54 kcal/mole to 1.85 kcal/mole . We have found the distance of bond formation in the complex in the range of 1.907 Å to 2.103 Å, the bond angle in the range of 172.73° to 178.80°, and frequency shift in the range of -151.76 cm^{-1} to -85.99 cm^{-1}. The electron density(ρ) and laplacian of electron density($\nabla^2\rho$) at bond critical points for the $C_2H_5OH...H_2O$ complexes are analyzed in DFT, and different levels of approximation by using AIM All software.

List of Abbreviations

DFT..... Density Functional Theory

B3LYP..... Becke, 3-parameter, Lee-Yang-Parr

B. E. ..... Binding Energy

FEM..... Finite Element Method

ORD..... Optical Rotary Displacement

GTO..... Gaussian Type Orbital

HF..... Hartree-Fock

SCF..... Self-Consistent Field

ZPVE..... Zero Point Vibrational Energy

LDA..... Local Density Approximation

LSDA..... Local Spin Density Approximation

MP2..... Second Moller Plesset

MP..... Moller Plessset

SCRF..... Self-Consistent Reaction Field

List of Figures

List of Tables

Contents

Chapter 1

Introduction

1.1 General Review

Two forces are responsible for keeping and holding the atoms and molecules united to form a stable system. They are intra-molecular and intermolecular forces. Covalent, ionic, and metallic bonds are due to intramolecular forces between the atoms within the molecule. Intermolecular forces play a significant role in the physical and chemical properties of crystal structures and molecular molecules. van der Waals forces, hydrogen bonds, and dipole-dipole interactions are three typical intermolecular force [1].

1.2 Hydrogen bond

The electronegative attractive interaction between polar molecules in which hydrogen(H) is bonded to highly electronegative atoms [F, O, N] is termed a hydrogen bond [2]. It is weaker than covalent or ionic bonds and stronger than van der Waals interaction. In the present context, its importance has been recognized in many fields like; material science, chemistry, and physics [3]. The definition of hydrogen bond proposed by the International Union of Pure and Applied Chemistry is "The hydrogen bond is an attractive interaction between an atom or a group of atoms in the same or a different molecule that shows the bond formation, and a hydrogen atom from a molecule or a molecular fragment X-H in which X is more electronegative than H"[4]. A hydrogen bond may be expressed as X-H ... Y-Z, where X-H represents the

hydrogen bond donor and the acceptor may be either an atom or an anion Y, or a fragment or a molecule Y−Z. Some useful shreds of evidence and characteristics for hydrogen bonding in this recommendation are given below;

- Electrostatic forces, which result from charge transfer between the donor and acceptor and lead to the partial covalent bond formation between H and Y, are among the factors involved in the creation of a hydrogen bond.
- The normal X-H...Y angle is linear (180°), and the closer the angle is to this value, the stronger the hydrogen bond and the shorter the H...Y distance.
- The frequency of the infrared X...H stretching typically shifts to the red when a hydrogen bond forms, lengthening the X...H bond.
- The atoms X and H are covalently connected to one another, with the strength of the H-Y bond increasing as X's electronegativity rises [4].

1.3 Scope of Present Work

The *ab initio* calculations are getting more popular in studying the electronic structure and calculating the several physical features such as ground state energy, dipole moment, vibrational frequency, geometry, topological analysis, polarizability, nuclear quadrupole, electric field gradient parameters, etc. We have worked on hydrogen bonding to study and analyze the different properties of ethanol and water complex using the Gaussian 16 program [5].

Water is the quintessential example of hydrogen bonding. We all know how important water is in our lives. Water is discern as a natural solvent. Without hydrogen bonds, water would not be formed in the liquid phase. So hydrogen bonding is crucial for sustaining life. Hydrogen bonding is used to determine the structure of various substance like protein. Most of our food, including carbohydrates and sugar, contains hydrogen bonds. So we have worked on hydrogen bonding to study and analyze the different properties of ethanol and water complex. Many chemical reactions depend on hydrogen bonding, which also gives water its special solvent properties. Hydrogen bonds are responsible for establishing the three-dimensional structure of

folded proteins, including enzymes and antibodies, and they hold complementary strands of DNA together [6].

Chapter 2

Literature Review and Motivation

Numerous researchers have studied interactions on various compounds using both experimental and computational methods. We have read the following literature's during our study because it gives a clear understanding of our research effort.

Rabuck and Scuseria (2000) were able to accurately finding the hydrogen bond binding energy and equilibrium structure for a benchmark set of molecules compared to newly developed functional [7].

Dkhissi *et al.* (2000) studied the comparison between the calculated and experimental rotational constants for monomeric pyridine increases in the order DFT(B3PW91), DFT(B3LYP). This comparison allows them to conclude that DFT with the B3PW91 and B3LYP functionals are the best methods to study monomeric nucleic acid bases [8].

Oliveira and Vasconcellos (2006) studied the structures of the alcohol and water hydrogen complexes, which were fully optimized using B3LYP/ccp-VDZ calculations. The authors evaluated the theory using a set of criteria developed in terms of the CHELPG atomic charges and topological parameters of the atoms in the molecules theory [9].

Pal and Kundu (2012) studied the hydrogen bond formation in trimethylene glycol (TMG) water complexes. Authors applied the Hartree-Fock (HF) method, MP2

method, and density functional theory with dispersion functionals (DFT-D) using the 6-31++G(d,p) basis set [10].

Parajuli and Arunan (2015) studied the first principles of X-H...C and C-H...X hydrogen bonds in n-alkane-HX complexes (X = F, OH, alkane = propane, butane, pentane) and has been carried out using an *ab-initio* and density functional theory [11].

Zhao *et al.* (2016) studied the spectroscopic characteristics of water-methanol complexes containing aromatic rings as acceptors, such as benzene and 1,3,5-triaminobenzene. Four DFT functionals B3LYP, M062X, WB97XD, and B3LYPD3 were used to derive the complex's optimal geometries [12].

G C and Parajuli (2016) studied the first principles of ethanol complexes with H_2S, H_2O, and HF molecules and has been carried out using an MP2 level of theory [13].

2.1 Motivation

Much research has been done in the field of computational quantum chemistry using the Gaussian software to study the properties of molecules. Many chemical reactions depend on hydrogen bonding, which also gives water its special solvent properties. Hydrogen bonds are responsible for establishing the three-dimensional structure of folded proteins, including enzymes and antibodies, and they hold complementary strands of DNA together. Due to these reasons, we were highly motivated to conduct our research work.

2.2 Objective

Our goal is to present a thorough computational analysis utilizing density functional theory to understand the electronic nature of the hydrogen bond formation in the ethanol-water complex and its features. Understanding the fundamentals of hydrogen bond formation will be made easier by this study. The following parameters of

complexes are studied in this research work:

- To find bond length and bond angle of complex.
- To find binding energy of the complex.
- To find zero point energy of the complex.
- To study vibrational frequency shift of complex.
- To study topological analysis of complex.

Chapter 3

Theoretical Background

3.1 The Hartree-Fock Approximation

3.1.1 General Review

Every system of either solids or clusters are made up of mutually interacting electrons and nuclei, as well as the dynamics of these particles. It cannot be treated independently in general. Due to interactions between electrons and nuclei, calculating the eigen function in many body situations is difficult. To address the limitations of the Hartree Self Consistent Field Method, V. Fock adopted this revised technique to multi-particle system solution. The wave functions' anti-symmetric character is appropriately taken into account. Each electron in the system flows under the combined average field of the nucleus and other electrons, according to this method. This method of determining the wave function and energy of a stationary quantum multi-particle system is an approximation. For solving the Schrodinger equation, this method works for atoms, molecules, nanostructures, and solids [14].

3.1.2 Born-Oppenheimer Approximation

In quantum physics, there are only a few exact solutions to problems of atoms. The Born-Oppenheimer approximation is one of the main concepts that guides the description of the quantum states of molecules. The motion of the nuclei and the motion of the electrons may be separated using this approach. The most used mathematical approximation in molecular dynamics is the Born-Oppenheimer (BO) approxima-

tion. The Born-Oppenheimer approximation is a hypothesis in quantum physics and molecular chemistry that the motion of the nuclei in a multi-electron system may be completely separated from the motion of the electron. Max Born and J. Robert Oppenheimer develop this approach in 1927. It is a significant idea in the quantum exploration of atoms, molecules, and other objects i.e. a molecule's wave function may be totally separated into electronic and nuclear (vibrational, rotational) components. The Born-Oppenheimer approximation is a hypothesis in quantum physics and molecular chemistry that the motion of the nuclei in a multi-electron system may be completely separated from the motion of the electron[14].

The total wavefunction can be expressed as

$$\psi_{total} = \psi_{electronic} \times \psi_{nuclear} \tag{3.1}$$

If the nucleus and electron are assumed to be point masses without taking into account their spin-orbit relativistic interactions, the molecular Hamiltonian operator is written as

$$\hat{H} = -\frac{\hbar^2}{2}\sum_{\alpha}\frac{1}{m_\alpha}\nabla_\alpha^2 - \frac{\hbar^2}{2m_e}\sum_i \nabla_i^2 + \sum_\alpha \sum_{\beta>\alpha} \frac{Z_\alpha Z_\beta e^2}{4\pi\epsilon_o r_{\alpha\beta}} - \sum_\alpha \sum_i \frac{Z_\alpha e^2}{4\pi\epsilon_o r_{i\alpha}} + \sum_j \sum_{i>j} \frac{e^2}{4\pi\epsilon_o r_{ij}} \tag{3.2}$$

where i,j represent the number of electrons, ϵ_o= 8.85×10 $^{-12}$ C^2/Jm is the permittivity of space and α,β refers to nuclei. In atomic units i.e, e = m$_e$ = 1).

The Hamiltonian is formally defined as

$$\hat{H} = \hat{T}_N(R) + \hat{T}_e(R) + \hat{V}_{NN}(R) + \hat{V}_{eN}(r,R) + \hat{V}_{ee}(r) \tag{3.3}$$

where nuclear coordinates are denoted by R and electronic coordinates by r, respectively.

In equation (3.2), the electron kinetic energy operator is represented by the first term, and the nuclei kinetic energy operator is represented by the second term. The potential energy of attraction between electrons and nuclei is represented by the third term. The potential energy of repulsion between nuclei with the atomic numbers Zα and Zβ is represented by the fourth term. The third factor on the right-hand side of the equation prevents us from clearly separating the Hamiltonian into its electronic and nuclear components. A nucleus has a mass that is significantly greater than that of a proton. By applying this approximation, we can ignore the nuclear kinetic

energy term in the equation (3.2) and it written as

$$(\hat{H}_{el} + V_{NN})\psi_{el} = U\psi_{el} \tag{3.4}$$

where $\hat{H}_{el}$ is the purely electronic Hamiltonian and V_{NN} is the nuclear repulsion term are expressed as

$$\hat{H}_{el} = -\frac{\hbar^2}{2m_e}\sum_i \nabla_i^2 - \sum_\alpha \sum_i \frac{Z_\alpha e^2}{4\pi\epsilon_o r_{i\alpha}} + \sum_j \sum_{i>j} \frac{e^2}{4\pi\epsilon_o r_{ij}} \tag{3.5}$$

$$V_{NN} = \sum_\alpha \sum_{\beta>\alpha} \frac{Z_\alpha Z_\beta e^2}{4\pi\epsilon_o r_{\alpha\beta}} \tag{3.6}$$

The electronic energy in equation (3.5) is referred to as total energy U as it includes inter-nuclear repulsion. Since the electronic wave function $\psi_{el}(r_i,r_\alpha)$ is just a function of electronic coordinates, it still depends on nuclear coordinates parametrically. Through the potential V_{eN}, both the electronic energy and the electronic wave function are parametrically dependent on the nuclear coordinates r_α (which implies we have distinct electronic Schrodinger equations with different solutions for different sets of fixed nuclear coordinates r_α).

Generally,

$$\psi_{el} = \psi_{el,n}(q_i, q_\alpha) \tag{3.7}$$

$$U = U_n(q_\alpha) \tag{3.8}$$

The electronic quantum number is denoted by the letter n. For a definite nuclear configuration, the term V_{NN} in equation (3.5) is a constant (say C). As a result, it has no effect on the wave function and simply reduces the energy eigenvalues by C. As a result, if V_{NN} is left out of equation (3.5), we obtain

$$\hat{H}_{el}\psi_{el} = E_{el}\psi_{el} \tag{3.9}$$

Where, the purely electronic energy $E_{el}(q_\alpha)$ is related to the electronic energy including internuclear repulsion by the relation

$$U = E_{el} + V_{NN} \tag{3.10}$$

Because electrons travel at a considerably higher rate than nuclei, When the nuclei alter their configuration slightly, say from q'_α to q''_α, the electrons adjust by changing the electronic wave function from $\psi_{el}(q_i;q'_\alpha)$ to $\psi_{el}(q_i;q''_\alpha)$ and the electronic

energy from U($q\prime_\alpha$) to U($q\prime\prime_\alpha$). As a result, as the nuclei move, the electronic energy fluctuates smoothly as a function of the nuclear configuration parameters, and U(q_α) becomes the potential energy for nuclear motion. This is the prime approximation in the Born-Oppenheimer approximation method, often known as the adiabatic approximation. Hence, the schrodinger equation for nuclear motion is

$$\hat{H}_N \psi_N = E_N \psi_N \tag{3.11}$$

$$\hat{H}_N = -\frac{1}{2} \sum_\alpha \frac{1}{m_\alpha} \nabla_\alpha^2 + U(q_\alpha) \tag{3.12}$$

The nuclear coordinates are denoted by q_α. Because the Hamiltonian (3.13) includes operators for both nuclear and electronic energy, the energy eigenvalue E in equation (3.12) represents the overall energy of the molecule. As a result, Electronic and nuclear movements are separated using the Born-Oppenheimer approximation, which suggests that the actual molecule wave function is

$$\psi(q_i, q_\alpha) = \psi_{el}(q_i; q - \alpha)\psi_N(q_\alpha) \tag{3.13}$$

if$(m_e/m_\alpha)^{1/4} \ll 1$.

3.1.3 Hartree-Self Consistent Field Method

Schrodinger equation for hydrogen and hydrogen similar atoms can be solved using precise wave function. The Hartree Method of Self-Consistent Field is the best way for finding the appropriate wave function for high order atoms [15]. This technique presupposes that each electron flows under the electrostatic field or effective potential created by the remaining electrons in a system. As a result, the many-body issue is reduced to a single-electron problem. The result is then generalized to the entire system. This is a technique for locating a centralÂ field. In the quantum realm, this approach is the foundation for using atomic and molecule orbitals in multi-electrode systems [3].

The Hamiltonian of an atom with a Z-charge nucleus and n electrons can be written as,

$$\hat{H} = -\frac{\bar{h}^2}{2m_e} \sum_{i=1}^{n} \nabla_i^2 - \sum_{i=1}^{n} \frac{Ze^2}{4\pi\epsilon_o r_i} + \sum_{i=1}^{n-1} \sum_{j=i+1}^{n} \frac{e^2}{4\pi\epsilon_o r_{ij}} \tag{3.14}$$

In this case, the nucleus was considered to have an indefinitely heavy point mass. The first sum in equation contains the kinetic energy operators for the n-electron

(3.14). The second sum is a representation of the potential energy for the interactions between the electrons and the Ze charge nucleus. For a neutral atom, Z=n. The potential energy of interelectronic repulsions is the final total. The constraint $j > i$ prevents phrases like $e^2/4\pi\epsilon_o r_{ij}$ from being counted twice for each interelectronic repulsion. The Schrodinger equation for an atom is inseparable due to the interelectronic repulsion factors $e^2/4\pi\epsilon_o r_{ij}$. If the Schrodinger equation could be separated, the n-hydrogen-like orbitals would give rise to the zeroth-order wave function.

$$\psi^o = f_1(r_1, \theta_1, \phi_1) f_2(r_2, \theta_2, \phi_2) ..... f_n(r_n, \theta_n, \phi_n) \tag{3.15}$$

where, hydrogen like orbitals are

$$f = R_{nl}(r) Y_l^m(\theta, \phi) \tag{3.16}$$

We would introduce two electrons with opposing spins into each of the atom's lowest orbitals in accordance with the Pauli exclusion principle, resulting in the ground-state configuration. Though the approximation wave function (3.16) is subjectively beneficial, it is woefully inaccurate numerically. For starters, all of the orbitals make use of the whole nuclear charge Z. We may achieve a better approximation to account for the screening of the electrons by utilizing different effective atomic numbers for the different orbitals. The next step is to apply a variation function that is similar to equation (3.16) but is not limited to hydrogen orbitals or any other type of orbitals. Thus we take

$$\phi = g_1(r_1, \theta_1, \phi_1) g_2(r_2, \theta_2, \phi_2) ..... g_n(r_n, \theta_n, \phi_n) \tag{3.17}$$

and we look for the functions $g\_1, g_2, ..., g_n$ that minimize the variational integral $<\phi|\hat{H}|\phi>/<\phi|\phi>$. In equation (3.16) we must vary the functions g_i. We employ orbitals that are created by multiplying a radical factor by a spherical harmonic to make the work easier.

$$g_i = h_i(r_i) Y_{li}^{mi}(\theta_i, \phi_i) \tag{3.18}$$

In most atomic computations, this approximation is used. The Hartree technique of self-consistent field, which was developed by Hartree in 1928, is the method for determining the g_i's .

$$\psi_o = S_1(r_1, \theta_1, \phi_1) S_2(r_2, \theta_2, \phi_2) ..... S_n(r_n, \theta_n, \phi_n) \tag{3.19}$$

Where, Each S_i is a multiplication of spherical harmonics and a normalized function of r. A plausible hypothesis for ϕ_o would be a combination of orbitals similar to those of hydrogen with effective atomic numbers for the function (3.20), and the probability density of electron 1 would be $|S_i|^2$. We'll start with electron 1 and imagine the remaining electrons 2, 3,..., n smeared out to produce a fixed distribution of electric charge across which electron 1 moves. The interaction between point charges Q_1 and Q_2 has a potential energy of $V_{12} = Q_1Q_2/4\pi\epsilon_o r_{12}$. Now we spread out Q_2 into a continuous charge distribution, where the charge density, or charge per unit volume represented by ρ_2. The infinitesimal charge in the infinitesimal volume $d\upsilon_2$ is $\rho_2 d\upsilon_2$, and when we add all the interactions between Q_1 and the microscopic charge components, we get

$$V_{12} = \frac{Q_1}{4\pi\epsilon_o}\int \frac{\rho_2}{r_{12}} d\upsilon_2 \tag{3.20}$$

The hypothetical charge cloud for electron 2 charge density is $\rho_2 = -e|s_2|^2$ and for electron 1, Q_1 = -e.

Thus,

$$V_{12} = \frac{Q_1}{4\pi\epsilon_o}\int \frac{|s_2|^2}{r_{12}} d\upsilon_2 \tag{3.21}$$

We obtain when we take into account interactions with other electrons.

$$V_{12} + V_{13} + ... + V_{1n} = \sum_{j=2}^{n} \frac{e^2}{4\pi\epsilon_o}\int \frac{|s_j|^2}{r_{1j}} d\upsilon_j \tag{3.22}$$

The potential energy of interaction between the nucleus and electron 1 and with the other electrons is then determined as

$$V_1(r_1, \theta_1, \phi_1) = \sum_{j=2}^{n} \frac{e^2}{4\pi\epsilon_o}\int \frac{|s_j|^2}{r_{1j}} d\upsilon_j - \frac{Zel^2}{r_1} \tag{3.23}$$

In addition to the presumption that the wave function is the sum of one electron orbital, we now make another approximation. We suppose that a function of r alone may effectively approximate the effective potential operating on an electron in an atom. The accuracy of this central field approximation may be demonstrated. As a result, we average $V_1(r_1, \theta_1, \phi_1)$ over the angles to get a potential energy that primarily depend on r_1.

$$V_1(r_1) = \frac{\int_0^{2\pi}\int_0^{\pi} V_1(r_1, \theta_1, \phi_1)\sin\theta_1 d\theta_1 d\phi_1}{\int_0^{2\pi}\int_0^{\pi}\sin\theta d\theta d\phi} \tag{3.24}$$

In a one-electron Schrodinger equation, we now take $V_1(r_1)$ as the potential energy,

$$\left[-\frac{\hbar^2}{2m_e}\nabla_1^2 + V_1(r_1)\right] t_1(1) = \epsilon_1 t_1(1) \tag{3.25}$$

Then determine $t_1(1)$, an orbital that will be more advantageous for electron 1. 1 is the energy of the orbital of the electron 1 in equation at this degree of approximation (3.26). Due to the potential energy's spherically symmetric nature in equation (3.25), the angular factor in t_1 is a spherical harmonic involving the quantum numbers l_1 and m_1. The radial component $R_1(r_1)$ in t_1 is obtained from the solution of a one-dimensional Schrodinger equation of the form equation (3.26) . The number of nodes k internal to the boundary points (r = 0 and ∞) starts at zero for the lowest energy and increases by 1 for each higher energy, yielding a set of solutions $R(r_1)$. Now, the definition of the quantum number n is given as n = l + 1 + k, where k = 0, 1, 2,... We have the same number of inner radial nodes (n-l-1) and the same orbitals (1s, 2s, 2p, and so on) as hydrogen-like atoms. The orbital energy also rises with n. Since $V_1(r_1)$ is not a straightforward Coulomb potential, the radial component $R_1(r_1)$ is not a hydrogen-like function.

From the collection of $R_1(r_1)$ solutions, we pick the one that matches the orbital we're optimizing. For instance, If electron 1 is a 1s electron in the beryllium $1s^2 2s^2$ configuration, we compute $V_1(r_1)$ from the assumed orbital of one 1s electron and two 2s electrons, then we utilize the radial solution of (3.26) with k = 0 to get a better 1s orbital.

We'll now examine electron 2 and visualize it passing through a dense charge cloud

$$-e\left[|t_1(1)|^2 + |s_3(3)|^2 + |s_4(4)|^2 + ... + |s_n(n)|^2\right] \tag{3.26}$$

As a result of the other electrons. To obtain an improved orbital $t_2(2)$, We solve the one-electron Schrodinger equation for electron 2 and calculate the effective potential energy $V_2(r_2)$. We repeat the operation until all n electrons have a set of enhanced orbitals. Then we go back to electron 1 and do it all over again. E keeps calculating better orbitals until there are no more changes from one iteration to the next. The Hartree self-consistent-field wave function is given by the last set of orbitals. By repeatedly resolving the one-electron Schrodinger equation (3.26), the orbital energy 1 was found. The energy of the repulsions between 1 and 2, 1 and 3,...,1 and n is included in the potential energy in (3.25). We are resolving a Schrodinger equation

for one electron with repulsions between electrons 2 and 1, 2 and 3,..., and 2 and n when we solve for 2. . Each interelectronic repulsion will be counted twice if we take $\sum_i \epsilon_i$. To accurately calculate the atom's total energy E, we must first calculate

$$E = \sum_{i=1}^{n} \epsilon_i - \sum_{i=1}^{n-1} \sum_{j=i+1}^{n} \int \int \frac{e^2 |g_i(i)|^2 |g_j(j)|^2}{4\pi\epsilon_o r_{ij}} d\upsilon_i d\upsilon_j \tag{3.27}$$

$$E = \sum_i \epsilon_i - \sum_i \sum_{j>i} J_{ij}$$

where the average repulsion of the electrons in the Hartree orbitals was calculated by subtracting the sum of the orbital energies (sth), and the notation J_{ij} was used for Coulomb integrals $\int \int \frac{e^2 |g_i(i)|^2 |g_j(j)|^2}{4\pi\epsilon_o r_{ij}} d\upsilon_i d\upsilon_j$.

3.1.4 Hartree-Fock Approximation

Hartree's self-consistent field approximation is one method for solving the Schrodinger equation in multi-electron systems. Each electron is supposed to travel freely in the effective field created by nuclei and remaining electrons in Hartree's self-consistent field technique, and each electron's motion is guided by a single particle Schrodinger equation [14]. For the N-electron problem, the Schrodinger wave equation is

$$H\psi(r_1, r_2, ..., r_N) = E\psi(r_1, r_2, ..., r_N) \tag{3.28}$$

where E stands for overall energy and H for the hamiltonian of the system. According to the Born approximation, the system's total Hamiltonian is given by,

$$H_{Tot} = -\frac{1}{2} \sum_i^N \nabla_i^2 + \frac{1}{2} \sum_{i \neq j}^N \frac{1}{|\mathbf{r_i} - \mathbf{r_j}|} - \sum_i^N \sum_I^M \frac{Z_I}{|\mathbf{r_i} - \mathbf{R_I}|} \tag{3.29}$$

The total wave function of an N-electrons system is calculated using the Hartree self consistent field approach as a simple multiple of one electron wave functions.

$$\psi(\mathbf{r_1}, \mathbf{r_2}, ..., \mathbf{r_N}) = \psi(\mathbf{r_1})\psi(\mathbf{r_2}).....\psi(\mathbf{r_N}) \tag{3.30}$$

Consequently, the total energy is given by,

$$
\begin{aligned}
E &= \langle\psi|H|\psi\rangle \\
&= \langle\psi| - \tfrac{1}{2}\textstyle\sum_i^N \nabla_i^2 + \tfrac{1}{2}\sum_{i\neq j}^N \frac{1}{|\mathbf{r_i}-\mathbf{r_j}|} - \sum_i^N \sum_I^M \frac{Z_I}{|\mathbf{r_i}-\mathbf{R_I}|}|\psi\rangle \\
&= \textstyle\int d^3r_1 \int d^3r_2 ..... \int d^3r_N \psi^*(r_1)\psi^*(r_2)....\psi^*(r_N) H \psi(r_1)\psi(r_2)....\psi(r_N) \qquad (3.31) \\
&= \textstyle\sum_{i=1}^N \int d^3\mathbf{r}\psi_i^*(\mathbf{r})(-\frac{1}{2}\nabla_i^2 - \sum_i \sum_I \frac{Z_I}{|\mathbf{r}_i-\mathbf{R}_I|}(\mathbf{r}))\psi_i(\mathbf{r}) \\
&+ \textstyle\sum_{i\neq j} \int d^3\mathbf{r} \int d^3\mathbf{r}' \psi_i^*(\mathbf{r})\psi_i(\mathbf{r})\frac{1}{|\mathbf{r}-\mathbf{r}'|}\psi_j^*(\mathbf{r}')\psi_j(\mathbf{r}')
\end{aligned}
$$

By reducing the Hartree energy (3.31) and applying the normalization condition, the electron wave function $\psi(r)$ can be derived,

$$I = \int \psi^*\psi d^3r = 1 \qquad (3.32)$$

using variational principle with respect to change in the orbital's i.e; $\psi_\mathbf{i}(\mathbf{r_i}) = \psi_\mathbf{i}(\mathbf{r_i}) + \delta\psi_\mathbf{i}(\mathbf{r_i})$. Using Langrange's indeterminate multiplier approach, we can do this. From variational principle

$$\delta(\langle\psi|H|\psi\rangle - \epsilon\langle\psi|\psi\rangle) = 0 \qquad (3.33)$$

$$
\begin{aligned}
&i.e. \delta(E-\epsilon I) = 0 \\
&= \textstyle\int d^3\mathbf{r}\delta\psi_i^*(\mathbf{r}) \left\{ \left(-\frac{1}{2}\nabla_i^2 - \sum_i \sum_I \frac{Z_I}{|\mathbf{r}_i-\mathbf{R}_I|} \right)\psi_i + \left(\int d^3\mathbf{r}' \frac{1}{|\mathbf{r}-\mathbf{r}'|} \sum_{i\neq j} \psi_i^*(\mathbf{r}')\psi_i(\mathbf{r}') \right)\psi_i - \epsilon\psi_i \right\} \\
&+ \textstyle\int d^3\mathbf{r}\delta\psi_i(\mathbf{r}) \left\{ \left(-\frac{1}{2}\nabla_i^2 - \sum_i \sum_I \frac{Z_I}{|\mathbf{r}_i-\mathbf{R}_I|} \right)\psi_i^* + \left(\int d^3\mathbf{r}' \frac{1}{|\mathbf{r}-\mathbf{r}'|} \sum_{i\neq j} \psi_j^*(\mathbf{r}')\psi_i^*(\mathbf{r}') \right)\psi_i^* - \epsilon\psi_i^* \right\}
\end{aligned}
\qquad (3.34)
$$

where ϵ denotes Lagrange's undetermined multiplier and $\delta\psi$, $\delta\psi*$ are variations in ψ and $\psi*$ absolutely unrelated to each other. From the previous equation for arbitrary $\delta\psi$ and $\delta\psi*$,we get,

$$\left(-\frac{1}{2}\nabla_i^2 - \sum_i \sum_I \frac{Z_I}{|\mathbf{r}_i-\mathbf{R}_I|} + \int d^3\mathbf{r}' \frac{1}{(|\mathbf{r}-\mathbf{r}'|)} \sum_{i\neq j} \psi_j^*(\mathbf{r}')\psi_j(\mathbf{r}') \right)\psi_i(\mathbf{r}) = \epsilon\psi_i(\mathbf{r}) \qquad (3.35)$$

$$\left(-\frac{1}{2}\nabla_i^2 + V_{ext} + V_{SC} \right)\psi_i(\mathbf{r_i}) = \lambda_i\psi_i(r_i) \qquad (i =, 2, ...N; \epsilon \to \lambda_i) \qquad (3.36)$$

where

$$V_{ext} = \sum_i \sum_I \frac{Z_I}{|\mathbf{r}_i - \mathbf{R}_I|}$$

and

$$\begin{aligned} V_{(sc)} &= V_H \\ &= \int d^3\mathbf{r}' \tfrac{1}{(|\mathbf{r}-\mathbf{r}'|)} \textstyle\sum_{i\neq j} \psi_j^*(\mathbf{r}')\psi_j(\mathbf{r}') \\ &= \int d^3\mathbf{r}' \tfrac{1}{(|\mathbf{r}-\mathbf{r}'|)} n_i(\mathbf{r}')n_i(\mathbf{r}') \\ &= \textstyle\sum_{j\neq i} |\psi_j^*(\mathbf{r}')|^2 \end{aligned}$$

The Hartree equation is the set of N-coupled integro-differential equations given in equation (3.36) that can be solved self-consistently.

The total wave function of an N-electron system is calculated using the Hartree self-consistent field approach as a simple product of one electron wave function ψ_i. It has at least one important flaw: The anti-symmetry principle states that a wave function describing fermions must be anti-symmetric in the space and spin coordinates of two electrons, and this action is in violation of that principle [14]. In order to fulfill the Pauli exclusion principle Hartree-Fock approximation employs the anti-symmetric wave function in the form of Slater determinant as given;

$$\psi = \frac{1}{\sqrt{N!}} \begin{vmatrix} \psi_1(\mathbf{r}_1, s_1) & \psi_2(\mathbf{r}_1, s_2) & \cdots & \psi_N(\mathbf{r}_1, s_N) \\ \psi_2(\mathbf{r}_2, s_1) & \psi_2(\mathbf{r}_2, s_2) & \cdots & \psi_N(\mathbf{r}_2, s_N) \\ \vdots & \vdots & & \vdots \\ \psi_N(\mathbf{r}_N, s_1) & \psi_N(\mathbf{r}_N, s_2) & \cdots & \psi_N(\mathbf{r}_N, s_N) \end{vmatrix} \tag{3.37}$$

where $\frac{1}{\sqrt{N!}}$ is a normalization constant and $\psi(r_i, s_i)$ is a single electron wave function with space and spin coordinates r_i and s_i. In addition, two electrons occupying the same spin-orbital create two identical rows, which results in the determinant equaling zero and obeying the Pauli exclusion principle. These two events are consistent with the wavefunction's antisymmetric feature.

By applying the wave function as given in (3.37) we can solve the Schrodinger equation applying variation principle which generates Hartree-Fock equation as follows;

$$\begin{aligned} &\left(-\tfrac{1}{2}\nabla_i^2 + V_{ext} + \int d^3\mathbf{r}' \tfrac{1}{(|\mathbf{r}-\mathbf{r}'|)} \textstyle\sum_{i\neq j} \psi_j^*(\mathbf{r}')\psi_j(\mathbf{r}')\right)\psi_i \\ &- \left(\int d^3\mathbf{r}' \tfrac{1}{|\mathbf{r}-\mathbf{r}'|} \textstyle\sum_{j\neq i} \psi_j^*(\mathbf{r}')\psi_i(\mathbf{r}')\delta_{s_i s_j}\right)\psi_j(\mathbf{r}) = \epsilon_i\psi_i(\mathbf{r}) \end{aligned} \tag{3.38}$$

The exchange potential V_{Exc}, which is non-local and connected to the interaction of every electrons in the system, is represented by the final term in the LHS of the preceding equation. As a result, deriving V_{Exc} is tough.

Although the Hartree-Fock wave function meets the Pauli's exclusion principle's anti-symmetry criteria and so contains the correlation effect originating from electrons with the same spin, the motion of electrons with opposing spins remains uncorrected. Within the Born-Oppenheimer approximation, this results in an electronic energy that does not equal the precise solution of the Schrodinger equation. To account for electron dynamic correlations, the Hartree-Fock (HF) approximation must be enhanced. DFT, MP2, and other approaches are utilized to account for dynamic electron correlation.

We present Roothaan's variational approach, which converts integro-diffierential equations into linear algebraic equations, in this brief description of the HF method.

3.1.5 Roothaan's Variational Method

The Roothaan variational method is used to express the spin orbitals as a linear combination of a small number of basis functions, and the integrodifferential equations for the functions $\Phi_i(\vec{x})$ are translated into linear algebraic equations for the expansion coefficient $c_{i\alpha}$. If we consider a finite basis set $\chi_\alpha(\vec{x})$ with N' linearly independent functions $\chi_1(\vec{x})$,$\chi_2(\vec{x})$.....,$\chi'_N(\vec{x})$, As a linear combination of the basis functions, the spin orbitals can be expressed as follows:

$$\Phi_i(\vec{x}) = \sum_{\alpha=1}^{N} c_{i\alpha}\chi_\alpha(\vec{x}) \tag{3.39}$$

where the expansion coefficient is $c_{i\alpha}$. The set of N' linearly independent functions may be used to generate the same number of atomic or molecular spin orbitals. If N is the number of occupied spin orbitals, then $N' \geq N$ is required. We have what is known as a minimum basis set when $N' = N$. Roothaan's technique, which is an extension of the LCAO (Linear Combination of Atomic Orbitals) approximation, may be easily applied to molecular systems.

With the help of equation(3.39) for $\Phi_i(\vec{x})$, the values of H_i, J_{ij} and K_{ij}, equations

are written in the forms ;

$$H_i = \sum_{\alpha,\beta} c_{i\alpha}^* c_{i\beta} \left[\alpha|\beta\right]$$
$$J_{ij} = \sum_{\alpha,\beta\gamma,\delta} c_{i\alpha}^* c_{i\beta} c_{j\gamma}^* c_{i\delta} \left[\alpha\beta|\gamma\delta\right]$$
$$K_{ij} = \sum_{\alpha,\beta\gamma,\delta} c_{i\alpha}^* c_{i\beta} c_{j\gamma}^* c_{i\delta} \left[\alpha\delta|\gamma\beta\right] \tag{3.40}$$

where,one-electron integrals are defined as follows:

$$\left[\alpha|\beta\right] = \int d\vec{x} \chi_\alpha^*(\vec{x}) \left(-\frac{1}{2}\nabla^2 - \sum_n \frac{Z_n}{|\ \vec{r}_n|} \right) \chi_\beta(\vec{x}) \tag{3.41}$$

Integrals with two electrons, such as;

$$\left[\alpha\beta|\gamma\delta\right] = \int\int d\vec{x} d\ \vec{x'} \chi_\alpha^*(\vec{x}) \chi_\beta(\vec{x}) \frac{1}{|\vec{r} - \ \vec{r'}|} \chi_\gamma^*(\ \vec{x'}) \chi_\delta(\ \vec{x'}) \tag{3.42}$$

According to the number of unique indices $\alpha, \beta, \gamma, \delta$, two-electron integrals are further classed as two-, three-, or four-center integrals. Unless the basis functions χ_α and χ_β have the same spin, the integrals produced by equations (3.41) and (3.42) disappear. We can deduce the following from equation (3.40);

$$E\left(c_{i\alpha}, c_{i\alpha}^*\right)) = \sum_i \sum_{\alpha\beta} c_{i\alpha}^* \left[\left[\alpha|\beta\right] + \frac{1}{2} \sum_j \sum_{\gamma\delta} C_{j\gamma}^* C_{j\delta} \left[\alpha\beta|\gamma\delta\right] - \left[\alpha\delta|\beta\gamma\right] \right] \tag{3.43}$$

For the energy expression's minimal value with respect to the variation of the coefficient $c_{i\alpha}$ under the orthonormalization condition;

$$\sum_{\alpha\beta} c_{i\alpha}^* c_{j\beta} S_{\alpha,\beta} = \delta_{ij} \tag{3.44}$$

With

$$S_{\alpha\beta} = \int d\vec{x} \chi_\alpha^*(\vec{x}) \chi_\beta(\vec{x})$$

We use Langrange's approach of undetermined multipliers to convert this conditional minimization to unconditional minimization. As a result, we define a functional as follows:

$$F\left(c_{i\alpha}, c_{i\alpha}^*\right) = E\left(c_{i\alpha}, c_{i\alpha}^*\right) - \sum_{ij} \lambda_{ij} \sum_{\alpha\beta} c_{i\alpha}^* c_{j\beta} S_{\alpha\beta} \tag{3.45}$$

where N^2 quantities λ_{ij} are known as Lagrange undetermined multipliers. For a closed shell system, the set of coefficients $c_{i\alpha}$ also diagonalizes the $\Lambda - matrix$ $[=(\lambda_{ji})]$ i.e., $\lambda_{ij} = \epsilon_i \delta_{ij}$.

When the minimization condition $\frac{\delta F}{\delta c^*_{i\alpha}} = 0$ is applied, we get:

$$\sum_i \sum_{\alpha\beta} \left[[\alpha|\beta] + \sum_i \sum_{\gamma,\delta} c^*_{j\gamma} c_{j\delta} \{ [\alpha\beta|\gamma\delta] - [\alpha\delta|\beta\gamma] \} - \epsilon_i S_{\alpha\beta} \right] c_{i\beta} = 0$$

Equivalently,

$$\sum_\beta \left(H_{\alpha\beta} - \epsilon_i S_{\alpha\beta} \right) c_{i\beta} = 0 \tag{3.46}$$

where $i = 1, 2, ..., N$ and $\alpha = 1, 2, ..., N'$. If we assume $\frac{\delta F}{\delta c^*_{i\alpha}} = 0$, the complex conjugates of equation (3.46) are obtained. The Rothaan's equations are algebraic versions of the Hartree-Fock equations and are known as the linear equation (3.46). The vanishing of the $N' \times N'$ secular determinant is required for non-trivial solutions of equation (3.46);

$$det \left(H_{\alpha\beta} - \epsilon_i S_{\alpha\beta} \right) = 0 \tag{3.47}$$

which has N' eigenvalues $\epsilon_i = \lambda_{ji}$ and N' sets of spin-orbital coefficients $c_{i\alpha}$. This diagonalization method differs from the general diagonalization process because the matrix element $H_{\alpha\beta}$ is dependent on the coefficient $c_{i\alpha}$. The $H_{\alpha\beta}$ must be recomputed and the secular equation must be solved until self consistency is achieved once the set $c_{i\alpha}$ is obtained at one stage of the calculation.

The occupied spin orbitals into the ground state correspond to the lowest N self consistent eigenvalues of the secular equation equation (3.47). The virtual solutions ϕ_i with $i = 1, 2, ..., N + 1$ to N' (for $N' > N$) correspond to the unoccupied spin orbitals and can be used to generate excited configurations. For virtual spin orbitals, ϵ_i is usually positive.

3.2 Electron Correlation Methods

3.2.1 General Review

Due to an overestimation of electron-electron repulsion, the HF technique provides "absolute"energies that are too high. Two different types of electron-electron repulsion exist: classical Coulomb repulsion (the Coulomb hole), which results from electric charge, and quantum mechanical repulsion (the Fermi hole), which exists between electrons with the same spin. The use of a single determinant and the "smeared electron cloud"integration used to obtain the J and K integrals result in the HF approximation to the treatment of electron correlation. It is common practice to refer to the shortcomings of the Hartree-Fock (single determinant) model as "electron correlation".

The average electron density for the other electron is used to compute the repulsion energy between two electrons in the Hartree-Fock model. This is unphysical because it ignores the reality that the electron will push the other electrons aside as it goes around. The repulsive energy is reduced as a result of the electrons' propensity to remain apart. First, explain why, given a sufficiently big and adaptable basis set, the Hartree-Fock approach is unable to provide the proper solution to the SchrĂśdinger equation. In passing, we point out that the "Hartree-Fock limit"refers to the best Hartree-Fock wave function that can be produced with a basis set that is this big and adaptable. The issue is that electron pairings do not take place as the Hartree-Fock technique predicts. It implies that the likelihood of the two electrons existing in the same region of space is the same as the likelihood of their existing in separate symmetry equivalent regions of space. For instance, in H_2, the probability of both electrons being close to one atom is the same as the likelihood of one electron being close to one atom and the other close to the second atom.

Clearly, this is incorrect. The repulsive energy is also only calculated using the Hartree-Fock method as an average throughout the entire molecular orbital. In actuality, the two electrons in a molecular orbital move so that they maintain a greater distance between one another than proximity. We refer to this outcome as "correlation". The "correlation energy"[3] is the energy difference between the exact result and the Hartree-Fock limit energy. Dynamical correlation refers to the idea of elec-

trons avoiding one another, but non-dynamical or static correlation energy refers to a subtler impact. Due to almost degenerate states or the rearrangement of electrons inside partially filled shells, nondynamical correlation energy demonstrates the inadequacy of a single reference in defining a particular molecular state. It is sometimes even more practical to divide the correlation energy into two components with distinct physical origins.

The majority of the correlation energy may be achieved for most excited states and chemical reactions where bonds are broken and formed by simply adding a few additional configurations in addition to the Hartree-Fock configuration. This portion of the correlation energy results from near degeneracy between various configurations and frequently originates in Hartree-Fock approximation artifacts. The dynamical correlation of the motion of the electrons, also known as the "dynamical correlation energy", is the physical source of the second component of the correlation energy. This portion of the correlation energy can be very accurately characterized by single and double replacements from the leading, near degenerate reference configurations since the Hamiltonian operator only contains one- and two-particle operators. It is crucial to take into account the electron correction, which is mostly brought on by the instantaneous interaction between electrons, in order to improve the HF approximation. The distinction between the precise ground state energy and the HF ground state energy (within the Born-Oppenheimer approximation and ignoring the relativistic effect) i.e. $\mathrm{E}_0 - \mathrm{E}_{HF}$ is called the correlation energy [16].

$$E_{corr} = E_o - E_{HF} \tag{3.48}$$

We briefly address the Moller-Plesset (MP2) perturbation, where the unperturbed wave function is the Hartree-Fock wave function, in order to take electron correlation effects into consideration.

3.2.2 Moller-Plesset(MP2) Perturbation Theory

In order to deal with systems with numerous interacting particles (nucleons in a nucleus, atoms in solids, electrons in an atom or molecule), physicists and chemists have devised a variety of perturbation-theory methods [3]. One approach to take

into account the electron correlation beyond the Hartree-Fock approximation is the Moller-Plesset perturbation theory. For a discussion of the Moller-Plesset perturbation theory, we follow Szabo and Ostlund [15]. In this theory, we partition the Hamiltonian as;

$$\hat{H} = \hat{H}_o + \hat{V} \tag{3.49}$$

Where $\hat{H} = \hat{H}_o + \hat{V}$ is the Hartree-Fock Hamiltonian for total electron system and is the sum of one electron Fock operators $f(i)$;

$$\hat{H}_o = \sum_i f(i) \tag{3.50}$$

$$= \sum_i [h(i) + V_{HF}(i)] \tag{3.51}$$

With $h(i)$ as a core-Hamiltonian for the i^{th} kinetic and potential energy of an electron in the field of a nucleus (the core) and $V_{HF}(i)$ as the Hartree-Fock potential. Let,$\hat{H}$ be the system's Hamiltonian is provided by ;

$$\hat{H} = \sum_i h(i) + \sum_{i<j} \frac{1}{|\ \vec{r}_{ij}|} \tag{3.52}$$

The difference between the total electron-electron repulsion and the total of the Hartree-Fock Coulomb and exchange potentials is known as the perturbation. Consequently, perturbation potential is ;

$$\hat{V} = \hat{H} - \hat{H}_o \qquad = \sum_{i<j} \frac{1}{|\ \vec{r}_{ij}|} - \sum_i V_{HF}(i) \tag{3.53}$$

This is the difference between the Hartree-Fock potentials and the overall electron-electron repulsion.

The Hartree-Fock wave-function $|\psi_o\rangle$ is an eigenfunction of $\hat{H}_o$, so that;

$$\hat{H}_o \psi_o\rangle = E_o^{(o)} \psi_o\rangle \tag{3.54}$$

With the eigenvalue;

$$E_o^{(o)} = \sum_\alpha \varepsilon_a \tag{3.55}$$

Where ϵ_α is the energy of the a^{th} orbital and hence $E_o^{(o)}$ is the zeroth-order perturbation energy. The Hartree-Fock energy is given by;

$$E_{HF} = \langle\psi_o|\hat{H}|\psi_o\rangle \tag{3.56}$$

Using the value of $\hat{H}$ from equation (3.49), we have;

$$E_{HF} = \langle\psi_o|\hat{V}|\psi_o\rangle \tag{3.57}$$

$$= \langle\psi_o|\ \hat{H}_o + \hat{V}|\psi_o\rangle + \langle\psi_o|\hat{V}|\psi_o\rangle \tag{3.58}$$

Multiplying equation (3.54) by $\langle\psi_o|$ and using the orthonormality condition $\langle\psi_o|\psi_o\rangle$ = 1, we get

$$E_o^{(o)} = \langle\psi_o|\ \hat{H}_o|\psi_o\rangle \tag{3.59}$$

Hence, with the aid of equation (3.56), equation (3.58) can be written as;

$$E_{HF} = E_o^{(o)} + E_o^{(1)} \tag{3.60}$$

where $E_o^{(1)} = \langle\psi_o|\hat{V}|\psi_o\rangle$ is defined as the first order energy correction. The Hartree-Fock energy is the result of adding the first and zeroth order energies together. The higher order perturbation theory provides the correlation energy. Similarly, the energy's second order adjustment is;

$$E_o^{(2)} = \sum_n \frac{|\langle\psi_o|\hat{V}|n\rangle|^2}{E_o^{(o)} - E_n^{(o)}} \tag{3.61}$$

Where the system's ground state is the only state over which the sum is applied and $|0\rangle = |\psi_o\rangle$ is the unperturbed wave-function, where, $|n\rangle$ is the perturbed wave function. Suppose that $|n\rangle$ be single excited determinant $|\psi_a^r\rangle$ constructed from $|\psi_o\rangle$ by replacing one occupied orbital χ_a with an unoccupied spin orbital χ_r. Then, we have;

$$\langle\psi_o|\hat{V}|n\rangle = \langle\psi_o|\hat{V}|psi_a^\gamma\rangle$$

$$= \langle\psi_o|\hat{H}|psi_a^r\rangle - \langle\psi_o|\ \hat{H}_o|psi_a^r\rangle \tag{3.62}$$

The R.H.S of equation (3.62) is zero since the first term vanishes according to Brillouin's theorem which states that the singly excited determinant does not interact directly with the Hartree-Fock (HF) determinant and the second because the spin

orbitals are eigenvalues of the Fock operator. Hence, $|n\rangle$ can not be singly excited state which do not mix with $|\psi_o\rangle$ because of the two particle nature of the perturbation. Thus, we are left with double excitation of the form $|\psi_{ab}^{rs}\rangle$. In this case, equation (3.61) can be written as;

$$E_o^{(2)} = \sum_{a<b,r<s} \frac{|\langle\psi_o|\hat{V}|\psi_{ab}^{rs}\rangle|^2}{E_o^{(o)} - E_{ab,rs}^{(o)}} \tag{3.63}$$

The doubly excited determinant $|\psi_{ab}^{rs}\rangle$ is an eigenfunction of H_0 and it can be constructed from $|\psi_o\rangle$ by replacing two occupied spin orbitals χ_a and χ_b with unoccupied spin orbitals χ_r and χ_s, so

$$\hat{H}_o|\psi_{ab}^{rs}\rangle = \left[E_0^{(o)} - (\varepsilon_a + \varepsilon_b - \varepsilon_r - \varepsilon_s)\right]|\psi_{ab}^{rs}\rangle \tag{3.64}$$

with an eigenvalue;

$$E_{ab,rs}^{(o)} = E_0^{(o)} - (\varepsilon_a + \varepsilon_b - \varepsilon_r - \varepsilon_s) \tag{3.65}$$

Thus, equation (3.63) can be written as;

$$E_o^{(2)} = \sum_{a<b,r<s} \frac{|\langle\psi_o|\hat{V}|\psi_{ab}^{rs}\rangle|^2}{\varepsilon_a + \varepsilon_b - \varepsilon_r - \varepsilon_s} \tag{3.66}$$

Let us evalaute the matrix element $\langle\psi_o|\hat{V}|\psi_{ab}^{rs}\rangle$. Putting the value of $\hat{V}$ from equation (3.64), we have;

$$\langle\psi_o|\hat{V}|\psi_{ab}^{rs}\rangle = \langle\psi_o|\sum_{i<j}\frac{1}{r_{ij}}|\psi_{ab}^{rs}\rangle - \langle\psi_o|\sum_i V_{HF}^i|\psi_{ab}^{rs}\rangle \tag{3.67}$$

The ground state N-electron Hartree-Fock determinant in terms of the anti-symmetrization operator is ;

$$|\psi_o\rangle = |\chi_a(1), \chi_b(2), \cdots, \chi_N(N) \quad = \frac{1}{N!}\sum_{i=1}(-1)^{p_i}P_i\{\chi_a(1), \chi_b(2), \cdots, \chi_N(N)\} \tag{3.68}$$

where is an operator which generates the i^{th} permutation of electron labelled 1, 2, ...N and p_i is the number of transposition (simple interchanges) required to obtain this permutation. Also, the doubly excited determinant $|\psi_{ab}^{rs}\rangle$ can be written as;

$$|\psi_{ab}^{rs}\rangle = |\chi_r(1), \chi_s(2), \cdots, \chi_c(N) \quad = \frac{1}{N!}\sum_{j=1}(-1)^{p_i}P_j\{\chi_r(1), \chi_s(2), \cdots, \chi_c(N)\} \tag{3.69}$$

And,

$$\langle\psi_o|\sum_{i<j}\frac{1}{r_{ij}}|\psi_{ab}^{rs}\rangle = \langle|(\frac{1}{r_{12}}+\frac{1}{r_{13}}+\cdots+\frac{1}{r_{N-1N}})|\psi_{ab}^{rs}\rangle \tag{3.70}$$

Each of the terms on right hand side of equation (3.70) gives the same result because of the indistinguishability of electrons and obtain.

$$\begin{aligned}\langle\psi_o|\sum_{i<j}\frac{1}{r_{ij}}|\psi_{ab}^{rs}\rangle &= \frac{N(N-1)}{2}\langle\psi_o|\sum_{i<j}\frac{1}{\tau_{12}}|\psi_{ab}^{rs}\rangle \\ &= \frac{N(N-1)}{2}\frac{1}{N!}\sum_{i=1}^{N!}\sum_{j=1}^{N!}(-1)^{p_i}(-1)^{p_j}\int d\ \vec{x}_1 d\vec{x_2}\cdots d\vec{x_N} \\ &\left[P_i\{\chi_a^*(1)\chi_b^*(2)\cdots\}\vec{r_{12}^{-1}}P_j\{\chi_r(1)\chi_s(2)\cdots\}\right]\end{aligned} \tag{3.71}$$

If the electrons labelled χ_r and χ_s be two spin orbitals occupied by two electrons labelled as 1 and 2 respectively in the permutation P_i, then there are two possibilities for electrons labelled 1 and 2 in the permutation P_j.

If $P_i\chi_r(1)\chi_s(2)...=\ ,\chi_r(1)\chi_s(2)...$, then;

$$P_j\{\chi_r(1)\chi_s(2)\cdots\} = \{\chi_r(1)\chi_s(2)\cdots\} or \{\chi_s(1)\chi_r(2)\cdots\}$$

Consider P_{12} is an exchange operator which interchanges the co-ordinates of electrons labelled 1 and 2, then we can write;

$$P_j\{\chi_r(1)\chi_s(2)\cdots\} = (1-P_{12})P_i\{\chi_r(1)\chi_s(2)\cdots\}$$

Then, equation(3.71)can be written as;

$$\begin{aligned}\langle\psi_o|\sum_{i<j}\frac{1}{r_{ij}}|\psi_{ab}^{rs}\rangle = \frac{1}{2(N-2)!}\sum_{i=1}^{N!}\int d\vec{x}_1 d\vec{x}_2\cdots d\vec{x}_N \\ P_i\{\chi_a^*(1)\chi_b^*(2)\cdots\}r_{12}^{-1}(1-P_{12})P_i\{\chi_r(1)\chi_s(2)\cdots\}\end{aligned}$$

where the two terms arise from placing electrons labelled 1 and 2 in χ_a and χ_b or χ_b and χ_a. Interchanging two dummy variables in equation (3.70), we get;

$$\begin{aligned}\langle\psi_o|\sum_{i<j}\frac{1}{r_{ij}}|\psi_{ab}^{rs}\rangle &= \int d\vec{x}_1 d\vec{x}_1\left[\chi_a^*(1)\chi_b^*(2)r_{12}^{-1}\chi_r(1)\chi_s(2)\right] \\ &= \langle ab|r_{12}^{-1}|rs\rangle - \langle ab|r_{12}^{-1}|sr\rangle \\ &= \langle ab|rs\rangle\end{aligned} \tag{3.72}$$

On substitution of equation (3.72) in equation (3.70), we get;

$$E_o^{(2)} = \sum_{a<b,r<s} \frac{|\langle ab|rs\rangle|^2}{\varepsilon_a + \varepsilon_b - \varepsilon_r - \varepsilon_s} \tag{3.73}$$

Then, the ground state energy corrected up to the second -order is given in the form;

$$\begin{aligned} E_o &= E_o^{(o)} + E_o^{(1)} + E_o^{(2)} \\ &= E_{HF} + E_o^{(2)} \end{aligned} \tag{3.74}$$

Equation (3.74) provides the energy value calculated at the MP2 level of approximation. The value of $E_o^{(2)}$ in equation (3.66) is always negative and hence the ground state energy is lower than the Hartree-Fock energy. As the MP method is not variational, the MP2 values of energy may be overcorrected [16].

3.3 Density Functional Theory (DFT)

3.3.1 General Review

The central difficulty in many-body systems is to calculate the total energy of a real system made up of N interacting electrons in a given external field v_{ext}, which is the nuclei's coulomb potential. The total energy of a system is calculated using the density of electrons in the density functional approach. In other words, the electron density is the primary variable under consideration. In other words the basic variables treated is the electron density. As Hamiltonian of the many body depends upon the total number of electrons and so is the electron density, this leads to the idea of expressing the total energy in terms of the electron density. In addition to total number of electrons, calculating gradient of electron density $(\frac{\partial n(\vec{r})}{\partial \vec{r}})$ the position of the nuclei in the system can be found out by using the Kato's cusp condition $(\frac{\partial n(\vec{r})}{\partial \vec{r}})|_{\vec{r}=0} = -2Zn(\vec{r}=0))$ for a nuclear site in the ground state of any atom, molecule or solid. Knowing the electron density one can found out total number of electrons in the system and the total number of the nuclei and hence define the Hamiltonian. The density functional methods of Thomas and Fermi define an unstable molecule relative to their dissociation into it's constituents. The main establishment of the method came into effect after the Hohenberg-Kohn theorem and

Kohn-Sham approach [3,17]. They demonstrated how the electron density may be used to calculate the energy of an interacting system. Therefore, the Hohenberg-Kohn theorem forms the core of the density functional theory [3].

3.3.2 Density Functional Theory

Density Functional Theory(DFT) is a theory that allows to replace the complicated N-electron wave function ($\psi(r_1, r_2.....r_N)$) and the associated Schrodinger equation by the much simpler variable, the electron density $\rho(\mathbf{r})$ [18].

The electronic Hamiltonian of a many-electron system can be expressed as the following using the Born-Oppenheimer approximation:

$$\hat{H} \quad = \quad \hat{T} + \hat{V}_{ne} + \hat{V}_{ee} \tag{3.75}$$

Where the first term represents the kinetic energy of an electron, the second term their nuclei's attraction, and the third term their Coulomb repulsion. The second portion of equation (3.75) for the N electrons and M nuclei system can be expressed as

$$\mathbf{V}_{ne} \quad = \quad \sum_{i=1}^{N}\sum_{n=1}^{M}\frac{Z_n}{|\mathbf{r}_i - \mathbf{R}_n|} = \sum_{i=1}^{N} V_{ext}(\mathbf{r}_i) \tag{3.76}$$

where $V_{ext}(\mathbf{r}_i) = \sum_{n=1}^{M}\frac{Z_n}{|\mathbf{r}_i - \mathbf{R}_n|}$ is known as external potential on the i^{th} electron due to M nuclei present in the system. With this Hamiltonian, The source of the ground state energy is

$$E_0 \quad = \quad \langle\psi_0|\hat{T}|\psi_0\rangle + \langle\psi_0|\hat{V}_{ne}|\psi_0\rangle + \langle\psi_0|\hat{V}_{ee}|\psi_0\rangle = T + V_{ne} + V_{ee} \tag{3.77}$$

where $|\psi_0\rangle$ is the N-electron system's ground state wave function.

According to the first Hohenberg-Kohn theorem [19], the ground state electron density is the basic variable and it uniquely determines the Hamiltonian operator that characterizes the system's ground state. The external potential $V_{ext}(\mathbf{r})$ is (within a constant) a unique functional of this ground state electron density. Equation (3.77)

can be written as, since the ground state energy in an external potential $V_{ext}(\mathbf{r})$ is a functional of the ground state electron density $\rho_0(\mathbf{r})$

$$E_0[\rho_0] = T[\rho_0] + V_{ne}[\rho_0] + V_{ee}[\rho_0] \tag{3.78}$$

with the average external potential V_{ne} is given as

$$V_{ne} = \langle\psi_0| \sum_{i=1}^{N} V_{ext}(\mathbf{r}_i)|\psi_0\rangle = \int \rho_0(\mathbf{r}) V_{ext}(\mathbf{r}) d\mathbf{r}.$$

Then, equation(3.78) takes the form

$$E_0[\rho_0] = \int \rho_0(\mathbf{r}) V_{ext}(\mathbf{r}) d\mathbf{r} + F[\rho_0] \tag{3.79}$$

Where the universal functional $F[\rho_0]$ is defined as

$$F[\rho_0] = T[\rho_0] + V_{ee}[\rho_0]. \tag{3.80}$$

The functional $F[\rho_0]$ is independent of the system's external potential and contains the total of the functionals for kinetic energy and electron-electron interaction.

According to second Hohenberg-Kohn theorem [3, 19] states that $F[\rho_0]$, the functional that transfer the ground state energy of the system, transfers the lowest energy if and only if the input density is the true ground state density ρ_0 i.e. for every trial density function $\rho(\mathbf{r})$ that satisfies $\int \rho(\mathbf{r}) = N$ and $\rho(\mathbf{r}) \geq 0$ for all $\mathbf{r}$, the following inequality holds:

$$E_0 = E[\rho_0] \leq E[\rho(\mathbf{r})]. \tag{3.81}$$

For any arbitrary electron density $\rho(\mathbf{r})$, the Hohenberg-Kohn functional $F[\rho(\mathbf{r})]$ in relation to this variable density, is the sum of the kinetic energy and the electron-electron repulsion operator with the ground state wave function ψ. i.e.

$$F[\rho] = T[\rho(\mathbf{r})] + V_{ee}[\rho(\mathbf{r})] = \langle\psi|\mathbf{T} + \mathbf{V}_{ee}|\psi\rangle \tag{3.82}$$

with $|\psi|^2 = \rho$. The explicit form of the functional $F[\rho(\mathbf{r})]$ is not known as the explicit forms of $T[\rho(\mathbf{r})]$ and $V_{ee}[\rho(\mathbf{r})]$ are not known. However, the electron-electron

interaction energy V_{ee} can be split into two terms : the classical term $J[\rho(\mathbf{r})]$ and non-classical term $E_{ncl}[\rho(\mathbf{r})]$ as

$$V_{ee} = \frac{1}{2}\int\int \frac{\rho(\mathbf{r})\rho(\mathbf{r}')}{|\mathbf{r}-\mathbf{r}'|}d\mathbf{r}d\mathbf{r}' + E_{ncl}[\rho(\mathbf{r})] = J[\rho(\mathbf{r})] + E_{ncl}[\rho(\mathbf{r})] \quad (3.83)$$

Here, the non-classical contribution to the electron-electron interaction i.e. $E_{ncl}[\rho(\mathbf{r})]$ contains all the effects of self-interaction, exchange and Coulomb correlations. If the explicit form of $F[\rho]$ is known exactly, the ground state energy in a given potential can be calculated by minimizing a three-dimensional density function functional. The preceding discussion demonstrates that there is a distinct mapping between ground state electron density and ground state energy. As the explicit forms of functional are not known and the Hohenberg-Kohn theorem do not provide any procedure to determine these functionals, we follow Kohn and Sham approach to determine the unknown functionals. We now consider a non-interacting artificial reference system for which the expression for the total Hamiltonian is given by

$$\mathbf{H}_s = -\frac{1}{2}\sum_{i=1}^{N}\nabla_i^2 + \sum_{i=1}^{N}V_s(\mathbf{r}) \quad (3.84)$$

where N is the number of non-interacting electrons in the reference system and $V_s(\mathbf{r})$ is a 'local effective potential'. Because the exact wave functions of non-interacting electrons in non-degenerate states are Slater determinants, the Hamiltonian operator's ground state wave function given by (3.84) can be represented as

$$\phi_s = \frac{1}{\sqrt{N!}}\begin{vmatrix} \phi_1(\mathbf{x}_1) & \phi_2(\mathbf{x}_1) & .. & .. & \phi_N(\mathbf{x}_1) \\ \phi_1(\mathbf{x}_2) & \phi_2(\mathbf{x}_2) & .. & .. & \phi_N(\mathbf{x}_2) \\ .. & .. & .. & .. & .. \\ \phi_1(\mathbf{x}_N) & \phi_2(\mathbf{x}_N) & .. & .. & \phi_N(\mathbf{x}_N) \end{vmatrix} \quad (3.85)$$

The spin orbitals ϕ_is are termed as Kohn-Sham orbitals and are given by

$$\mathbf{F}_{ks}\phi_i = \epsilon_i\phi_i \quad (3.86)$$

where,

$$\mathbf{F}_{ks} = -\frac{1}{2}\nabla^2 + V_s(\mathbf{r})$$

is the Kohn-Sham operator with one electron and ϵ_is are Kohn-Sham orbital energies unlike the molecular orbital energies. The Kohn-Sham orbitals ϕ_i are electron orbitals

for a hypothetical reference system with no interaction between the electrons. With the right effective local potential $V_s(\mathbf{r})$, the artificial non-interacting reference system can be coupled to the actual interacting system so that the exact ground state electron density of the reference system is equal to the ground state electron density of the real system, i.e.

$$\rho_s(\mathbf{r}) = \sum_{i=1}^{N} |\phi_i(\mathbf{r})|^2 = \rho_0(\mathbf{r}) \tag{3.87}$$

The expression can be used to calculate the kinetic energy of the reference system that is not interacting but has the same density as the actual interacting system

$$T_s = -\frac{1}{2}\sum_{i=1}^{N}\langle\phi_i|\nabla^2|\phi_i\rangle \tag{3.88}$$

The following separation for the functional $F[\rho(\mathbf{r})]$ can be used to explain why the kinetic energy (T_s) of non-interacting systems differs from the actual kinetic energy (T_s) of real interacting systems

$$F[\rho(\mathbf{r})] = T_s[\rho(\mathbf{r})] + J[\rho(\mathbf{r})] + E_{xc}[\rho(\mathbf{r})] \tag{3.89}$$

where $E_{xc}[\rho(\mathbf{r})]$ is the exchange-correlation energy functional.From equations (3.82) and (3.89), we have

$$\begin{aligned} E_{xc}[\rho(\mathbf{r})] &= (T[\rho(\mathbf{r})] - T_s[\rho(\mathbf{r})]) + (V_{ee}[\rho(\mathbf{r})] - J[\rho(\mathbf{r})]) \\ &= T_c[\rho(\mathbf{r})] + E_{ncl}[\rho(\mathbf{r})] \end{aligned} \tag{3.90}$$

where $E_{ncl}[\rho(\mathbf{r})]$ is the non-classical contribution to the electron-electron interaction and $T_c[\rho(\mathbf{r})]$ is the remaining portion of the real kinetic energy that is not covered by (T_s). The non-classical effect of self interaction correction, exchange, and correlation on the system's potential energy as well as some kinetic energy are all contained in the exchange-correlation energy functional $E_{xc}[\rho(\mathbf{r})]$. The kinetic energy (T_s) and the energy resulting from the interaction with the external potential $V_{ext}(\mathbf{r})$ are the only two terms in the energy expression of a system that is not interacting $\rho(\mathbf{r})$. Hohenberg-Kohn theorems stipulate that the total energy must be a function of electron density $\rho(\mathbf{r})$. Therefore, T_s has to be a functional of electron density $\rho(\mathbf{r})$. Consequently, the reference system's overall energy can expressed as

$$E[\rho] = T_s[\rho] + \int \rho(\mathbf{r}) V_{ext}(\mathbf{r}) d\mathbf{r} \tag{3.91}$$

In terms of Kohn-Sham orbitals ϕ_i, we have

$$E[\phi_i^*, \phi_i] = -\frac{1}{2}\sum_{i=1}^{N}\langle\phi_i|\nabla^2|\phi_i\rangle + \sum_{i=1}^{N}\int |\phi_i(\mathbf{r})|^2 V_{ext}(\mathbf{r}) d\mathbf{r} \tag{3.92}$$

As the minimization of $E[\phi_i^*, \phi_i]$ in equation (3.92) is conditional, we make the conditional minimization to unconditional with the aid of Langrange's undetermined multipliers method. For this, we define a functional $G[\phi_i^*, \phi_i]$ as

$$G[\phi_i^*, \phi_i] = E[\phi_i^*, \phi_i] - \sum_i \epsilon_i \int \phi_i(\mathbf{r})^* \phi_i(\mathbf{r}) d\mathbf{r} \tag{3.93}$$

where ϕ_i^* and ϕ_i are treated as independent functional variables and ϵ_i denote the Langrange's multipliers.From equations (3.92) and (3.93), we have

$$\begin{aligned} G[\phi i^*, \phi_i] &= -\frac{1}{2}\sum_{i=1}^{N}\int \phi_i^*(\mathbf{r})\nabla^2\phi_i(\mathbf{r}) + \sum_{i=1}^{N}\int \phi_i^*(\mathbf{r}) V_{ext}(\mathbf{r})\phi_i(\mathbf{r}) d\mathbf{r} - \sum_i \epsilon_i \int \phi_i^*(\mathbf{r})\phi_i(\mathbf{r}) d\mathbf{r} \\ &= \sum_i \int \phi_i^*(\mathbf{r})\Big[-\frac{1}{2}\nabla^2 + V_{ext}(\mathbf{r}) - \epsilon_i\Big]\phi_i(\mathbf{r}) \end{aligned} \tag{3.94}$$

Taking the variation of G with respect of ϕ_i^* and ϕ_i, we get

$$\begin{aligned} \delta G[\phi_i^*, \phi_i] &= \sum_i \int \delta\phi_i^*(\mathbf{r})\Big[-\frac{1}{2}\nabla^2 + V_{ext}(\mathbf{r}) - \epsilon_i\Big]\phi_i(\mathbf{r}) d\mathbf{r} \\ &\quad + \sum_i \int \phi_i^*(\mathbf{r})\Big[-\frac{1}{2}\nabla^2 + V_{ext}(\mathbf{r}) - \epsilon_i\Big]\delta\phi_i(\mathbf{r}) d\mathbf{r} \end{aligned} \tag{3.95}$$

For the minimum value of G, we have δG=0,

$$\Big[-\frac{1}{2}\nabla^2 + V_{ext}(\mathbf{r})\Big]\phi_i(\mathbf{r}) = \epsilon_i\phi_i(\mathbf{r}), \quad i = 1, 2, ..., N \tag{3.96}$$

and its complex conjugate. The single-particle Schrondinger equation for the non-interacting reference system is represented by equation (3.96).

The energy expression for a real interacting system can now be written as

$$E[\rho(\mathbf{r})] = T_s[\rho(\mathbf{r})] + J[\rho(\mathbf{r})] + E_{xc}[\rho(\mathbf{r})] + V_{ext}[\rho(\mathbf{r})] \tag{3.97}$$

Writing explicit forms for $J[\rho(\mathbf{r})]$ and $V_{ext}[\rho(\mathbf{r})]$, equation (3.97) can be expressed as

$$\begin{aligned} E[\rho(\mathbf{r})] &= T_s[\rho(\mathbf{r})] + \frac{1}{2}\int\int \frac{\rho(\mathbf{r})\rho(\mathbf{r}')}{|\mathbf{r} - \mathbf{r}'|} d\mathbf{r} d\mathbf{r}' + E_{xc}[\rho(\mathbf{r})] \\ &+ \int \rho(\mathbf{r}) V_{ext}(\mathbf{r}) d\mathbf{r} \end{aligned} \tag{3.98}$$

In terms of Kohn-Sham orbitals ϕ_i and ϕ_i^*, equation (3.98) can be written as

$$\begin{aligned} E[\phi_i^*, \phi_i] &= -\frac{1}{2}\sum_{i=1}^{N}\langle\phi_i|\nabla^2|\phi_i\rangle + \frac{1}{2}\sum_{i=1}^{N}\sum_{j}\int\int |\phi_i(\mathbf{r})|^2 \frac{1}{|\mathbf{r}-\mathbf{r}'|}|\phi_j(\mathbf{r}')|^2 d\mathbf{r}d\mathbf{r}' + E_{xc}[\rho(\mathbf{r})] \\ &\quad + \sum_{i=1}^{N}\int \phi_i^*(\mathbf{r})V_{ext}(\mathbf{r})\phi_i(\mathbf{r})d\mathbf{r} \end{aligned} \tag{3.99}$$

The conditional minimization of energy functional E as given in equation(3.99) can be made equivalent to an unconditional one by the application of Langrange's method of undetermined multipliers as

$$G[\phi_i^*, \phi_i] = E[\phi_i^*, \phi_i] - \sum_i \epsilon_i \int \phi_i(\mathbf{r})^*\phi_i(\mathbf{r})d\mathbf{r} \tag{3.100}$$

where, ϕ_i^* and ϕ_i are treated as independent functional variables and ϵ_i denote the Langrange's multipliers.

With the aid of equation (3.99), equation(3.100) can be expressed as

$$\begin{aligned} G[\phi_i^*, \phi_i] &= -\frac{1}{2}\sum_{i=1}^{N}\langle\phi_i|\nabla^2|\phi_i\rangle + \frac{1}{2}\sum_{i=1}^{N}\sum_{j}\int\int |\phi_i(\mathbf{r})|^2 \frac{1}{|\mathbf{r}-\mathbf{r}'|}|\phi_j(\mathbf{r}')|^2 d\mathbf{r}d\mathbf{r}' + E_{xc}[\rho(\mathbf{r})] \\ &\quad + \sum_{i=1}^{N}\int \phi_i^*(\mathbf{r})V_{ext}(\mathbf{r})\phi_i(\mathbf{r})d\mathbf{r} - \sum_i \epsilon_i \int \phi_i(\mathbf{r})^*\phi_i(\mathbf{r})d\mathbf{r} \end{aligned} \tag{3.101}$$

The variation of $G[\phi_i^*, \phi_i]$ with respect to functional dependence on $\phi_i(\mathbf{r})$ and $\phi_i^*(\mathbf{r})$ is given by

$$\begin{aligned} \delta G[\phi_i^*, \phi_i] &= \delta\Big[-\frac{1}{2}\sum_{i=1}^{N}\langle\phi_i|\nabla^2|\phi_i\rangle\Big] + \delta\Big[\frac{1}{2}\sum_{i=1}^{N}\sum_{j}\int\int |\phi_i(\mathbf{r})|^2 \frac{1}{|\mathbf{r}-\mathbf{r}'|}|\phi_j(\mathbf{r}')|^2 d\mathbf{r}d\mathbf{r}'\Big] \\ &\quad + \delta E_{xc}[\rho(\mathbf{r})] + \delta\Big[\sum_{i=1}^{N}\int \phi_i^*(\mathbf{r})V_{ext}(\mathbf{r})\phi_i(\mathbf{r})d\mathbf{r}\Big] \\ &\quad - \delta\Big[\sum_i \epsilon_i \int \phi_i(\mathbf{r})^*\phi_i(\mathbf{r})d\mathbf{r}\Big] \end{aligned} \tag{3.102}$$

As $\rho(\mathbf{r}) = \sum_{i=1}^{N}\int \phi_i^*(\mathbf{r})\phi_i(\mathbf{r})d\mathbf{r}$, the variation in $\rho(\mathbf{r})$ is given by

$$\delta\rho(\mathbf{r}) = \sum_{i=1}^{N}\int \Big[\delta\phi_i^*(\mathbf{r})\phi_i(\mathbf{r}) + \phi_i^*(\mathbf{r})\delta\phi_i(\mathbf{r})\Big]d\mathbf{r} \tag{3.103}$$

Also, the variation in the exchange energy can be expressed as

$$\begin{aligned} \delta E_{xc}[\rho(\mathbf{r})] &= \frac{\delta E_{xc}[\rho(\mathbf{r})]}{\delta\rho(\mathbf{r})}\delta\rho(\mathbf{r}) \\ &= \frac{\delta E_{xc}[\rho(\mathbf{r})]}{\delta\rho(\mathbf{r})}\sum_{i=1}^{N}\int \Big[\delta\phi_i^*(\mathbf{r})\phi_i(\mathbf{r}) + \phi_i^*(\mathbf{r})\delta\phi_i(\mathbf{r})\Big]d\mathbf{r} \end{aligned} \tag{3.104}$$

With the aid of equations (3.102) and (3.104), equation (3.102) can be expressed as

$$\begin{aligned}\delta G[\phi_i^*,\phi_i] &= \sum_{i=1}^{N}\int \delta\phi_i^*(\mathbf{r})\Big[-\frac{1}{2}\nabla^2+V_{ext}+\frac{\delta E_{xc}[\rho(\mathbf{r})]}{\delta\rho(\mathbf{r})}-\epsilon_i\Big]\phi_i(\mathbf{r})d\mathbf{r}\\ &+\sum_{i=1}^{N}\int \phi_i^*(\mathbf{r})\Big[-\frac{1}{2}\nabla^2+V_{ext}+\frac{\delta E_{xc}[\rho(\mathbf{r})]}{\delta\rho(\mathbf{r})}-\epsilon_i\Big]\delta\phi_i(\mathbf{r})d\mathbf{r}\\ &+\frac{1}{2}\sum\sum\int\int d\mathbf{r}d\mathbf{r}'\Big[\delta\phi_i^*(\mathbf{r})\phi_j^*(\mathbf{r}')+\phi_i^*(\mathbf{r})\delta\phi_j^*(\mathbf{r}')\Big]\frac{1}{|\mathbf{r}-\mathbf{r}'|}\phi_i(\mathbf{r})\phi_j(\mathbf{r}')\\ &+\frac{1}{2}\sum\sum\int\int d\mathbf{r}d\mathbf{r}'\phi_i^*(\mathbf{r})\phi_j^*(\mathbf{r}')\frac{1}{|\mathbf{r}-\mathbf{r}'|}\Big[\delta\phi_i(\mathbf{r})\phi_j(\mathbf{r}')+\phi_i(\mathbf{r})\delta\phi_j(\mathbf{r}')\Big]\end{aligned} \tag{3.105}$$

Using equation (3.87) and the property of dummy variables, equation (3.105) can be written as

$$\begin{aligned}\delta G[\phi_i^*,\phi_i] &= \sum_{i=1}^{N}\int \delta\phi_i^*(\mathbf{r})\Big[-\frac{1}{2}\nabla^2+V_{ext}+\frac{\delta E_{xc}[\rho(\mathbf{r})]}{\delta\rho(\mathbf{r})}+\int\frac{\rho(\mathbf{r}')}{|\mathbf{r}-\mathbf{r}'|}d\mathbf{r}'-\epsilon_i\Big]\phi_i(\mathbf{r})d\mathbf{r}\\ &+\sum_{i=1}^{N}\int \phi_i^*(\mathbf{r})\Big[-\frac{1}{2}\nabla^2+V_{ext}+\frac{\delta E_{xc}[\rho(\mathbf{r})]}{\delta\rho(\mathbf{r})}+\int\frac{\rho(\mathbf{r}')}{|\mathbf{r}-\mathbf{r}'|}d\mathbf{r}'-\epsilon_i\Big]\delta\phi_i(\mathbf{r})d\mathbf{r}\end{aligned} \tag{3.106}$$

Setting $\delta G[\phi_i^*,\phi_i]=0$, we get

$$\Big[-\frac{1}{2}\nabla^2+V_{ext}+\frac{\delta E_{xc}[\rho(\mathbf{r})]}{\delta\rho(\mathbf{r})}+\int\frac{\rho(\mathbf{r}')}{|\mathbf{r}-\mathbf{r}'|}d\mathbf{r}'\Big]\phi_i=\epsilon_i\phi_i$$

$$\texttt{or,}\quad \Big[-\frac{1}{2}\nabla^2+V_{eff}(\mathbf{r})\Big]\phi_i=\epsilon_i\phi_i,\quad i=1,2.....,N \tag{3.107}$$

where $V_{eff}(\mathbf{r})=V_{ext}(\mathbf{r})+\dfrac{\delta E_{xc}[\rho(\mathbf{r})]}{\delta\rho(\mathbf{r})}+\displaystyle\int\frac{\rho(\mathbf{r}')}{|\mathbf{r}-\mathbf{r}'|}d\mathbf{r}'$ is the effective potential which depends on the density (i.e. one-electron orbitals) through Coulomb term. The set of N-coupled equations given by equation(3.107) and their complex conjugates are known as Kohn-Sham one-electron equations.

Comparing equation(3.107) with (3.86), we find that the effective potential $V_{eff}(\mathbf{r})$ is identical to the local potential $V_s(\mathbf{r})$ i.e.

$$V_s(\mathbf{r}) = V_{eff}(\mathbf{r})=V_{ext}(\mathbf{r})+V_{xc}(\mathbf{r})+\int\frac{\rho(\mathbf{r}')}{|\mathbf{r}-\mathbf{r}'|}d\mathbf{r}' \tag{3.108}$$

where $V_{xc}(\mathbf{r})$ is the potential due to the exchange-correlation energy and is given by

$$V_{xc}(\mathbf{r}) = \frac{\delta E_{xc}}{\delta\rho} \tag{3.109}$$

The Kohn-Sham potential, which is typically a local potential, is another name for the exchange-correlation potential $V_{xc}(\mathbf{r})$. The exchange-correlation potential, however, is nonlocally dependent on density for a genuine system. The exchange-correlation energy functional $E_{xc}[\rho(\mathbf{r})]$ for slowly shifting electron density $\rho(\mathbf{r})$ may be thought of as solely depending on the local value of the density $\rho(\mathbf{r})$ and not its gradients [3]. The local density approximation is what is used in this (LDA). To roughly express this, we can write

$$E_{xc}^{LDA}[\rho(\mathbf{r})] = \int \rho(\mathbf{r})\mathtt{E}_{xc}[\rho(\mathbf{r})]d\mathbf{r} \tag{3.110}$$

where $\mathtt{E}_{xc}[\rho(\mathbf{r})]$ is the hypothetical uniform electron gas's exchange and correlation energy per electron $\rho(\mathbf{r})$. Separating the quantity $\mathtt{E}_{xc}[\rho(\mathbf{r})]$ results in

$$\mathtt{E}_{xc}[\rho(\mathbf{r})] = \mathtt{E}_{x}[\rho(\mathbf{r})] + \mathtt{E}_{c}[\rho(\mathbf{r})] \tag{3.111}$$

The exchange functional $\mathtt{E}_{x}[\rho(\mathbf{r})]$ which represents the exchange energy of an electron in a uniform electron gas is defined as

$$\mathtt{E}_{x}[\rho(\mathbf{r})] = -\frac{3}{4}\left[\frac{3}{\pi}\right]^{\frac{1}{3}}[\rho(\mathbf{r})]^{\frac{1}{3}} \tag{3.112}$$

Slater exchange is the usual name for the exchange functional equation (3.112). The correlation part $\mathtt{E}_{c}[\rho(\mathbf{r})]$ has no explicit expressions. On the basis of findings from numerical quantum Monte-Carlo simulations of the homogeneous electron gas, a number of analytical formulations for $\mathtt{E}_{c}[\rho(\mathbf{r})]$ have been developed. For implementation, Vosko-Wilk-Nussair(VWN) correlation functional is the expression for $\mathtt{E}_{c}[\rho(\mathbf{r})]$ that is most frequently utilized. Thus, in LDA, SVWN approximates $\mathtt{E}_{xc}[\rho(\mathbf{r})]$ by identifying $\mathtt{E}_{xc}[\rho(\mathbf{r})]$ and representing the combination of the Slater exchange and VWN correlation functionals. Closed shell (restricted) systems with spin compensation correspond to this approximation [3].

For open shell system with unequal number of spin up α and spin down β electrons, the exchange energy functional depends not only upon the electron density $\rho(\mathbf{r})$ but

also depends upon the spin densities $\rho_\alpha(\mathbf{r})$ and $\rho_\beta(\mathbf{r})$ with $\rho_\alpha(\mathbf{r}) + \rho_\beta(\mathbf{r})$=$\rho(\mathbf{r})$. The approximation in which the exchange-correlation energy functional is assumed to depend upon the spin densities is called Local Spin Density Approximation(LSDA), which is the extension of LDA to the unrestricted case. In this approximation, $E_{xc}[\rho(\mathbf{r})]$ can be written as

$$\mathtt{E}_{xc}^{LDA}[\rho_\alpha(\mathbf{r}), \rho_\beta(\mathbf{r})] \;=\; \int \rho(\mathbf{r})\mathtt{E}_{xc}[\rho_\alpha(\mathbf{r}), \rho_\beta(\mathbf{r})]d\mathbf{r} \tag{3.113}$$

With this approach, various molecular properties like equilibrium structure, harmonic frequencies or charge moments (dipole, quadrupole etc) can be explained. However, the calculation of bond energy values are rather poor [3]. Thus, improvement on LSDA calculation has to be incorporated. One of the approach is to take the gradients of the density into account in the exchange-correlation energy and is known as the gradient corrected exchange-correlation functionals. There are many gradient corrected exchange-correlation functionals. A widely used exchange-correlation functional is B3LYP: Beck's gradient corrected exchange functional:(B) and gradient corrected correlation functional of Lee, Yang and Parr:(LYP) [3, 18].

Chapter 4

Research Methodology

4.1 General Review

The geometry of an atom's orbitals is described by a set of functions known as a basis set. The molecule's orbitals and the full wave function are produced by the linear combination of the basis function and the angular function [3, 20] .

The finite element method and simplex method are popular linear programming algorithms used in mathematical optimization. This method divides N-dimensional space into small subsystems that can be explained through N-linear equations with matrices' properties. If we can solve one matrix using this approach, we can solve all of them. The new solution yields the same outcome as the previous iteration once all possible solutions have been found. This process is called convergence. Numerous iterations are typically needed because the original guess may be quite off from the true value. While the theoretical model affects the kind of computations that will be done on the matrices, the chosen basis set effects the accuracy of the estimations. The calculation is terminated when it converges, but conversion does not imply that the system has reached its minimum. The system's stability should be checked. We can obtain our required minimum by using the perturbation method on the stable system and recalculating [21]. The Gaussian software consists of a number of the pseudo potentials and basis sets. The smallest basis sets are STO-nG basis sets which consist of the single contraction of n GTO(Gaussian Type Orbitals) orbitals. There are also Pople basis set. This type of basis set uses only one basis function for

each core atomic orbital and a larger basis for the valence atomic orbitals [14] and hence also called split-valence basis set. A split valence basis set is the 3-21G basis set, for instance. Each core orbital in the 3-21G basis set is represented by a contraction of just one of the three GTO primitives, and each valence shell is described by a contraction of two GTO primitives and another with one GTO primitive [16].

4.2 Gaussian 16

Gaussian 16 [5], a computational application for modeling electronic structures. It can predict many properties of molecules and reactions, including:

- Molecular orbitals, energies, and structures.
- Optical rotations (ORD) and Multipole moments.
- Energies and structures of transition states.
- Bond and reaction energies.
- Vibrational frequencies, IR, and Raman (Pre-resonance & Resonance) spectra.
- Thermochemical analysis and NMR properties.
- Reaction pathways etc.

This program can calculate the model in the ground state or in an excited state as well as in a gas phase or solution. The most recent version of the Gaussian series of electrical structure algorithms is Gaussian 16. Chemists, chemical engineers, biochemists, physicists, and others have already started using this program for study in both well-established and recently-emerging areas of chemical interest. It was first published as Gaussian 70 in 1970 by John Pople and his research team at Carnegie Mellon University. The following revisions have been made: 76, 80, 82, 86, 88, 90, 92, 94, 98, 03, 09, and 16. It can be used to investigate molecules and events in a range of situations, including stable species and substances that are challenging or impossible to see experimentally, like transition structures and short-lived intermediates. Because of its many characteristics and the fact that it may be used to examine even

larger molecular systems and more fields of chemistry, we employ this version in our current research. All observable molecular properties in solution can be predicted by Gaussian 16, and calculations on both ground state and excited state systems, as well as on our proprietary n-layered Integrated Molecular Orbital and Molecular Mechanics models, may take solvation into account. Gaussian 16 self-consistent reaction field (SCRF) facility, a more advanced use of this solvation approach, is used to represent compounds in solution. Even the most difficult calculations are simple to set up and specify using Gaussian 16. We've listed a few of the characteristics that help to realize these objectives. Examples of optimization aids and limitations include fragments, wavefunction stability analysis, intuitive molecular orbitals, and others. The following extension is possible for the inputs for Gaussian 16, which we utilize in this work: Text file and.gjf file for the Gaussian input. An ASCII text file containing a succession of lines serves as the Gaussian 16 input. The basic structure of a Gaussian input file consists of the following sections:

- Link 0 Commands: Locate and name scratch files.
- Route section (# lines): Specify desired calculation type, model chemistry, and other options.
- Title section: Brief description of the calculation.
- Molecule specification: Specify molecular system to be studied.
- Optional additional sections: Additional input needed for specific job types.

Multiple Gaussian job may be combined within a single input file and we can perform both at the same time.

4.3 GaussView 6

A critical component of our research is the graphical representation of complexes. GaussView 6 is the most advanced and powerful graphical user interface available for Gaussian 16. This application allows us to build or import molecular structures, set up, launch, monitor, and control Gaussian calculations, and view the predicted results graphicallyâall without ever leaving the application. It can analyze various

features like energy, optimization, frequency, etc. via different methods and schemes as our requirement. One can use this method from simple to large and complex molecular systems. In this application, all the coordinates, theory, basis set, etc. can be selected instead of typing according to the job type. Users of Gaussian 16 benefit from three main features of Gaussview 6. Gaussview, for starters, features a sophisticated visualization feature that enables users to quickly draw in even very huge and complex molecules. Users may then rotate, translate, and zoom in on these molecules using standard mouse actions. Second, GaussView offers a simple method for configuring various Gaussian calculation types. For both common job types and advanced approaches like ONIOM, STQN transition structure optimizations (e.g., Opt=QST2/QST3), CASSCF calculations, periodic boundary conditions (PBC) calculations, and many more, it makes preparing complex input simple. Last but not least, GaussView enables us to visualize the output of Gaussian calculations. It can ingest common molecular file formats like PDB (Protein Data Bank) files in addition to these advantage. For this task, we employ the GaussView 6 version of the software [22]. Graphical representations of the gaussian results are available below.

- Optimized molecular structures, orbital structures.
- Electron density surfaces from any computed density.
- Electrostatic potential surfaces.
- Diatomic charges and dipole moments.
- Animation of the normal modes corresponding to vibrational frequencies.
- IR, Raman, NMR, VCD, and other spectra etc.

4.4 Basis Sets

The set of (nonorthogonal) one-particle functions used to construct molecular orbitals is referred to as the basis set. The fundamental mathematical formula used to describe the contours of an atom's orbitals is known as a basis set [3].
The electronic wave function is represented by the basis set of the Density Functional Theory. It converts the model's partial equations into algebraic equations that can be

efficiently implemented on a computer. It can be conceptualized as a linear mixture of STOs (Slater-type orbitals) [23]. STO-nG basis sets, which are composed of a single contraction of n GTO (Gaussian Type Orbitals) orbitals, are the smallest basis sets. These also go by the name of "pople basis sets". It is the most basic kind of basis set that can accommodate smaller molecules like H_2 or He. The basic set having more than one STO for the valence shell but only one STO for the core shell. Meaning that different valence shells of atomic orbitals correlate to different basic functions. As a result, it is also known as split-valence basis set. A split valence basis set is the 3-21G basis set, for instance. Each core orbital in the 3-21G basis set is defined by a single contraction of the three GTO primitives, while each valence shell is described by a contraction of two GTO primitives and one GTO primitive, respectively [24]. Particularly in the case of anion molecules with wider electron distributions, diffuse functions are employed to define the wave function far from the nucleus. The addition of polarization functions, marked by an asterisk (*), makes the wave functions more adaptable. The words "polarization basis function", "single plus", and "double plus"have the same definitions. A polarized basis set is shown by 3-21G*, and a diffuse function is shown by 6-31+G*. The addition of a set of "d"primitives to non-hydrogen atoms is indicated by a single asterisk (*), whereas the addition of "p"primitives to the hydrogen atom is indicated by a double asterisk (**) [25]. The following is a list of the basic sets utilized in this work:

- 6-311++G(d,p)
- 6-311++G(2d,2p)
- aug-cc-pVTZ

4.5 Quantum Theory of Atom in Molecules(AIM)

The Atom in Molecules (AIM) theory is a link between quantum mechanics and chemistry. The only theory that provides a powerful definition of the two cornerstones of chemistry, the atom and the bond, is Atoms in Molecules. Using the molecular wave function as a starting point, AIM All is a software program for doing quantitative and visual QTAIM (Quantum Theory of Atoms in Molecules) investigations

of molecular systems. Members of the research team led by Richard F.W. Baders created the theoretical calculations program known as Atoms in Molecules (AIM) [26]. The results of the AIM theoretical study qualitatively concur with the results of the ab-initio analysis. We search for bond critical sites between hydrogen and nitrogen using theoretical computations on the complexes using atoms in molecules (AIM). Additionally, AIM theory might offer a separate theoretical foundation for the hydrogen bond radius [27]. Using AIM All, we have calculated, ,

- Topology
- Laplacian of the charge density at the bond critical point.
- Charge density at the bond critical point.

Chapter 5

Results and Discussion

5.1 General Review

This section deals with the results and discussion of our works. We have obtained the optimized geometries of $C_2H_5OH...H_2O$ complexes and have done the following calculations.

- Some Geometrical Parameters (bond length, bond angle)
- Frequency Shift
- Binding Energy (B.E.)
- Zero Point Vibrational Energy (ZPVE).
- Topology Analysis

All the calculations have been performed in the density functional theory(DFT) [16] calculations designated by various functionals such as; B3LYP, WB97XD, M062X, N12SX, M11L, and MN12L levels of approximation using Gaussian 16 program [5]. We use 6-311++G(d,p), 6-311++G(2d,2p), and aug-cc-pVTZ basis sets in this calculation.

5.2 Geometry of Complex

The presence of hydrogen bonds in the complex is analyzed by the mean of geometry parameter. The separation between the hydrogen atom H and the basic donor

atom , length of the hydrogen bond, and bond angle in the DFT(B3LYP, WB97XD, M062X, N12SX, M11L, and MN12L) levels of approximation with the basis sets 6-311++G(d,p), 6-311++G(2d,2p), and aug-cc-pVTZ considered in the present work. In complex X-H...Y, based on Y...H bond length, A hydrogen bond is classified by [28, 29]:

- Very strong 1.2 Å to 1.5 Å
- Strong 1.5 Å to 2.2 Å
- Weak 2.0 Å to 3.0 Å.

On the basis of change in X−H length $R_{X...H}$ $\mathring{A}$, hydrogen bond is classified by [28, 29]:

- Very strong 0.05 Å to 0.2 Å
- Strong 0.01 Å to 0.05 Å
- Weak $<$ 0.01 Å.

In the IUPAC report of hydrogen bonding criteria, the X−H...Y hydrogen bond angle tends to lie between 110° and 180°. On the formation of hydrogen bonds, the length of the X-H bond typically increases[4].
The optimized geometeries of $C_2H_5OH...H_2O$ complex in different levels of approximation using basis sets 6-311++G(d,p), 6-311++G(2d,2p), and aug-cc-pVTZ are shown in the Figure 5.1 to Figure 5.18 below;

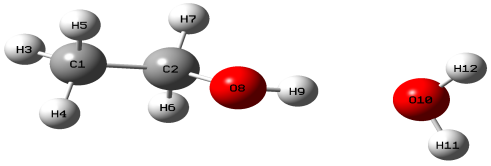

Figure 5.1: Structure of $C_2H_5OH...H_2O$ complex at B3LYP level of approximaton using 6-311++G(d,p) basis set.

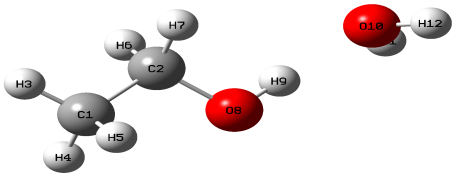

Figure 5.2: Structure of $C_2H_5OH...H_2O$ complex at WB97XD level of approximation using 6-311++G(d,p) basis set.

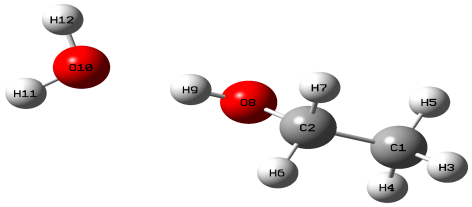

Figure 5.3: Structure of $C_2H_5OH...H_2O$ complex at M062X level of approximation using 6-311++G(d,p) basis set.

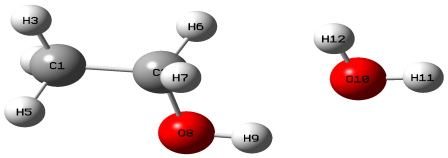

Figure 5.4: Structure of $C_2H_5OH...H_2O$ complex at N12SX level of approximation using 6-311++G(d,p) basis set.

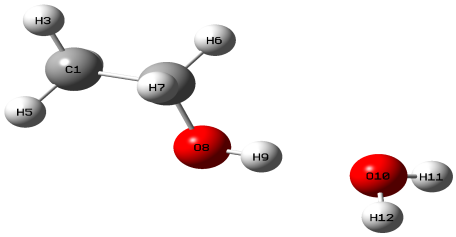

Figure 5.5: Structure of $C_2H_5OH...H_2O$ complex at M11L level of approximation using 6-311++G(d,p) basis set.

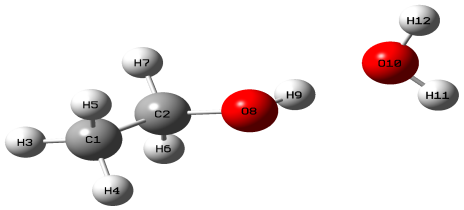

Figure 5.6: Structure of $C_2H_5OH...H_2O$ complex at MN12L level of approximation using 6-311++G(d,p) basis set.

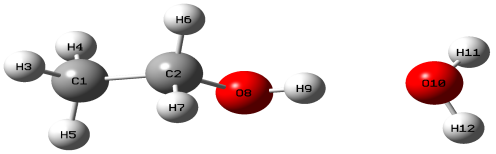

Figure 5.7: Structure of $C_2H_5OH...H_2O$ complex at B3LYP level of approximation using 6-311++G(2d,2p) basis set.

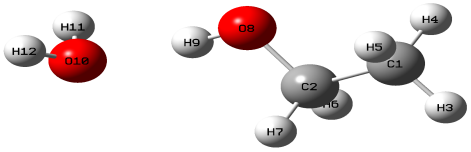

Figure 5.8: Structure of $C_2H_5OH...H_2O$ complex at WB97XD level of approximation using 6-311++G(2d,2p) basis set.

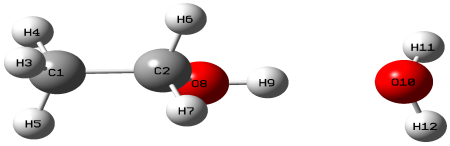

Figure 5.9: Structure of $C_2H_5OH...H_2O$ complex at M062X level of approximation using 6-311++G(2d,2p) basis set.

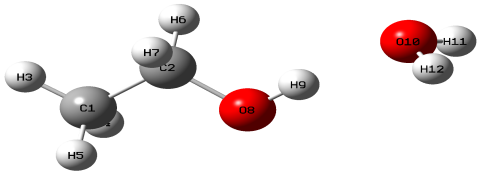

Figure 5.10: Structure of $C_2H_5OH...H_2O$ complex at N12SX level of approximation using 6-311++G(2d,2p) basis set.

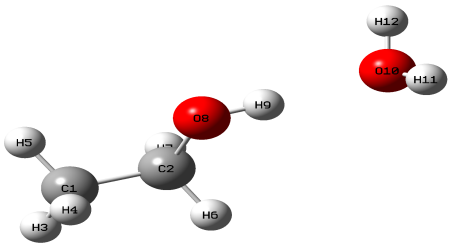

Figure 5.11: Structure of $C_2H_5OH...H_2O$ complex at M11L level of approximation using 6-311++G(2d,2p) basis set.

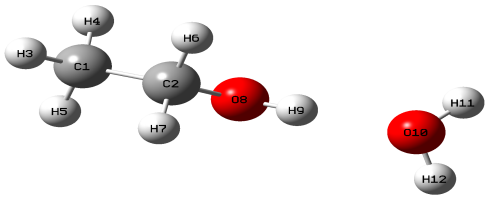

Figure 5.12: Structure of $C_2H_5OH...H_2O$ complex at MN12L level of approximation using 6-311++G(2d,2p) basis set.

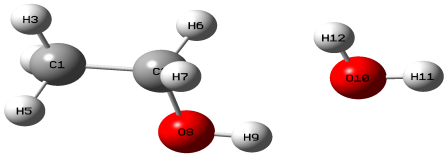

Figure 5.13: Structure of $C_2H_5OH...H_2O$ complex at B3LYP level of approximation using aug-cc-pVTZ basis set.

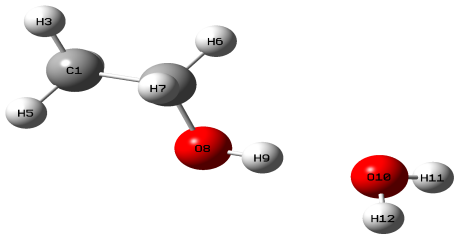

Figure 5.14: Structure of $C_2H_5OH...H_2O$ complex at WB97XD level of approximation using aug-cc-pVTZ basis set.

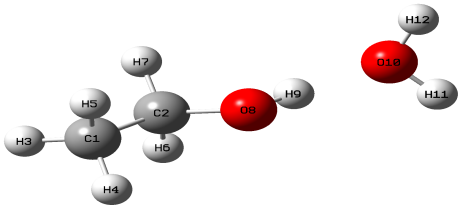

Figure 5.15: Structure of $C_2H_5OH...H_2O$ complex at M062X level of approximation using aug-cc-pVTZ basis set.

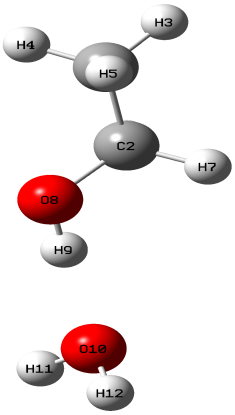

Figure 5.16: Structure of $C_2H_5OH...H_2O$ complex at N12SX level of approximation using aug-cc-pVTZ basis set.

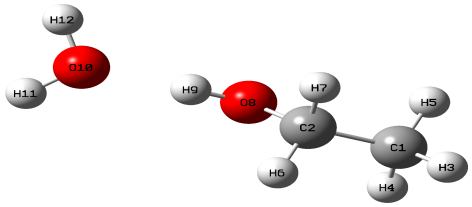

Figure 5.17: Structure of $C_2H_5OH...H_2O$ complex at M11L level of approximation using aug-cc-pVTZ basis set.

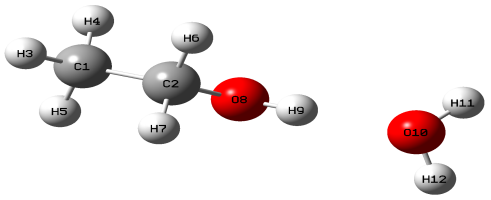

Figure 5.18: Structure of $C_2H_5OH...H_2O$ complex at MN12L level of approximation using aug-cc-pVTZ basis set.

We have studied the $C_2H_5OH...H_2O$ complex bond length (H9-O10) in DFT levels of approximation using 6-311++G(d,p) basis set which is shown in Table(5.1). From our calculations, we obtain that the hydrogen bond distance is minimum in $C_2H_5OH...H_2O$ (1.907Å) in M11L level of approximation and maximum in $C_2H_5OH...H_2O$ (1.976Å) in MN12L level of approximation. It shows that there is strong hydrogen bonding between ethanol and water, satisfying the bond formation length criteria given by the IUPAC report [4]. In addition, we have also compared our results with the observations of Oliveira and Vasconcellos, they carried out their observation in the basis set aug-cc-pVDZ at the DFT(B3LYP) level of approximation; their results are comparable to ours [9].

Table 5.1: Geometric features (bond length) of complex under different level of approximation by using 6-311++G(d,p) basis set.

S.N	Atom	level	Bond length (Å)
1	H9-O10	B3LYP	1.947
2	H9-O10	WB97XD	1.918
3	H9-O10	M062X	1.923
4	H9-O10	N12SX	1.909
5	H9-O10	M11L	1.907
6	H9-O10	MN12L	1.976

We have studied the $C_2H_5OH...H_2O$ complex bond length (H9-O10) in DFT levels of approximation using 6-311++G(2d,2p) basis set which is shown in Table(5.2). From our calculations, we obtain that the hydrogen bond distance is minimum in $C_2H_5OH...H_2O$ (1.928Å) in N12SX level of approximation and maximum in $C_2H_5OH...H_2O$ (2.010Å) in MN12L level of approximation. This shows that there is strong hydrogen bonding between ethanol and water, satisfying the bond formation length criteria given by the IUPAC report [4]. Moreover, we have also compared our results with the observations of Oliveira and Vasconcellos, they carried out their observation in the basis set aug-cc-pVDZ at the DFT(B3LYP) level of approximation; their results are comparable to ours [9].

Table 5.2: Geometric features (bond length) of complex under different level of approximation using 6-311++G(2d,2p) basis set.

S.N	Atom	level	Bond length (Å)
1	H9-O10	B3LYP	1.972
2	H9-O10	WB97XD	1.938
3	H9-O10	M062X	1.948
4	H9-O10	N12SX	1.928
5	H9-O10	M11L	1.934
6	H9-O10	MN12L	2.010

We have studied the $C_2H_5OH...H_2O$ complex bond length (H9-O10) in DFT level of approximation using basis set aug-cc-pVTZ which is shown in the Table(5.3). From our calculations, we obtain that the hydrogen bond distance is minimum in $C_2H_5OH...H_2O$ (1.930Å) in N12SX level of approximation and maximum in $C_2H_5OH...H_2O$ (2.103Å) in MN12L level of approximation. This shows that there is strong hydrogen bonding between ethanol and water, satisfying the bond formation length criteria given by the IUPAC report [4]. Furthermore, we have also compared our results with the observations of Oliveira and Vasconcellos, they carried out their observation in the basis set aug-cc-pVDZ at the DFT(B3LYP) level of approximation; their results are comparable to ours [9].

Table 5.3: Geometric features (bond length) of complex under different level of approximation using basis set aug-cc-pVTZ.

S.N	Atom	level	Bond length (Å)
1	H9-O10	B3LYP	1.968
2	H9-O10	WB97XD	1.937
3	H9-O10	M062X	1.944
4	H9-O10	N12SX	1.930
5	H9-O10	M11L	1.940
6	H9-O10	MN12L	2.103

We have also analyzed the angle $\angle OH...X(X = H_2O)$ of the complex in DFT levels of approximation with the choice of the basis set 6-311++G(d,p), the data is shown in Table (5.4), and the angle $\angle OH...X(X = H_2O)$ has maximum value of 178.80° at the M11L level of approximation for $C_2H_5OH...H_2O$ and minimum value of 173.59° at the M062X level of approximation for $C_2H_5OH...H_2O$ complex. We conclude that the complex shows hydrogen bonding with ethanol and water. Likewise, our results satisfy the angle criteria given by IUPAC report[4].

Table 5.4: Geometric features (bond angle) of complex under different level of approximation by using basis set 6-311++G(d,p).

S.N	Atom	level	Bond Angle (°)
1	O8-H9-O10	B3LYP	175.63
2	O8-H9-O10	WB97XD	177.90
3	O8-H9-O10	M062X	173.59
4	O8-H9-O10	N12SX	176.15
5	O8-H9-O10	M11L	178.89
6	O8-H9-O10	MN12L	177.06

We have also analyzed the angle $\angle OH...X(X = H_2O)$ of the complex in DFT levels of approximation with the choice of the basis set 6-311++G(2d,2p), the data is shown in the Table (5.5), and the angle $\angle OH...X(X = H_2O)$ has maximum value of 175.97° at the M11L level of approximation for $C_2H_5OH...H_2O$ and minimum value of 172.73°

at the B3LYP level of approximation for $C_2H_5OH...H_2O$ complex. We conclude that ethanol and water form hydrogen bonds with the complex. Additionally, our results satisfy the angle criteria given by IUPAC report [4].

Table 5.5: Geometric features (bond angle) of complex under different level of approximation by using basis set 6-311++G(2d,2p).

S.N	Atom	level	Bond Angle (°)
1	O8-H9-O10	B3LYP	172.73
2	O8-H9-O10	WB97XD	174.05
3	O8-H9-O10	M062X	174.37
4	O8-H9-O10	N12SX	173.06
5	O8-H9-O10	M11L	175.97
6	O8-H9-O10	MN12L	173.38

We have also analyzed the angle $\angle OH...X(X = H_2O)$ of the complex in DFT levels of approximation with the choice of the basis set aug-cc-pVTZ, the data is shown in the Table (5.6), and the angle $\angle OH...X(X = H_2O)$ has maximum value of 178.69° at the M11L level of approximation for $C_2H_5OH...H_2O$ and minimum value of 173.33° at the B3LYP level of approximation for $C_2H_5OH...H_2O$ complex . We infer that the complex, ethanol, and water form hydrogen bonds. Our results also satisfy the angle specifications given by IUPAC report [4].

Table 5.6: Geometric features (bond angle) of complex under different level of approximation by using basis set aug-cc-pVTZ.

S.N	Atom	level	Bond Angle (°)
1	O8-H9-O10	B3LYP	173.33
2	O8-H9-O10	WB97XD	174.74
3	O8-H9-O10	M062X	178.45
4	O8-H9-O10	N12SX	173.82
5	O8-H9-O10	M11L	178.69
6	O8-H9-O10	MN12L	173.77

5.3 Binding Energy

Binding energy is the minimum energy required to disrupt a stable nucleus, molecule, or atom into its constituent particles at infinite separation. The magnitude of the binding energy of a nucleus determines its stability against disintegration. If the binding energy is positive, the system is in the bound state that the nucleus is stable and energy must be supplied from outside to disrupt it into its constituents. If the binding energy is negative, the system is in an unbound state and it will disintegrate by itself.

According to Pauling, the range of typical hydrogen bond energy is 2-10 kcal/mol [2]. The IUPAC hydrogen bonding report does not specify a lower limit for hydrogen bonds but does suggest an upper limit of 5-6 kcal/mol [4].

According to Jiangang [28], Strengths of about 3-5 kcal/mol and typically less than 12 kcal/mol are regarded as normal hydrogen bonds. The proton is noticeably more tightly connected to one heavy element than the other members of such hydrogen bonds. This is the category that most neutral hydrogen bonds belong to. Energy levels for strong hydrogen bonding may be more than 12 kcal/mol. A short bond distance, a single minimum potential, or a double minimum with a very low barrier are characteristics of such strong hydrogen bonding. Significant covalent characteristics also exist in these bonds. A hydrogen bond is categorized according to its energy in kcal/mol as follows [28, 29]:

- Very strong -15 kcal/mol to -40 kcal/mol
- Strong -4 kcal/mol to -15 kcal/mol
- Weak < -4 kcal/mol

Binding Energies of complex can be calculated by using following relation:

Binding Energy = Energy of complex - Energy of monomers

In terms of eV, 1 hatree= 27.211 eV

In terms of kJ/mole, 1 hatree=2625.5 kJ/mole

In terms of kcal/mole, 1 hatree=627.5 kcal/mole [3].

We have studied the complex by using various functional with the choice of the basis set 6-311++G(d,p). We have calculated the binding energy. The binding energy are

in the range of -5.336 kcal/mol to -6.189 kcal/mol for the ethanol and water complex. We infer that the complex, ethanol, and water form hydrogen bonds. Our results also satisfy the angle specifications given by IUPAC report[4]. In the Table(5.9), it is clear that the value of binding energy for ethanol and water complex in various functional shows strong hydrogen bonds [29].

Table 5.7: Binding energies of complex in different levels of approximation using basis set 6-311++G(d,p)

Complex	Level	$B.E.^a$(Hartree)	$B.E.^b$ (kcal/mol)
$C_2H_5OH@H_2O$	B3LYP	-0.008654	-5.430
$C_2H_5OH@H_2O$	WB97XD	-0.009791	-6.143
$C_2H_5OH@H_2O$	M062X	-0.009933	-6.232
$C_2H_5OH@H_2O$	N12SX	-0.009863	-6.189
$C_2H_5OH@H_2O$	M11L	-0.008634	-5.417
$C_2H_5OH@H_2O$	MN12L	-0.008505	-5.336

We have studied the complex by using various functional with the choice of the basis set 6-311++G(2d,2p). We have calculated the binding energy (B.E). The binding energy are in the range of -4.590 kcal/mol to -5.340kcal/mol for the ethanol and water complex. We infer that the complex, ethanol, and water form hydrogen bonds. Our results also satisfy the angle specifications given by IUPAC report[4]. In the Table(5.8), it is clear that the value of binding energy for ethanol and water complex in various functional shows strong hydrogen bonds [29].

Table 5.8: Binding energies of complex in different levels of approximation using basis set 6-311++G(2d,2p)

Complex	Level	$B.E.^a$ (Hartree)	$B.E.^b$ (kcal/mol)
$C_2H_5OH@H_2O$	B3LYP	-0.007352	-4.613
$C_2H_5OH@H_2O$	WB97XD	-0.0081357	-5.105
$C_2H_5OH@H_2O$	M062X	-0.008454	-5.304
$C_2H_5OH@H_2O$	N12SX	-0.008511	-5.340
$C_2H_5OH@H_2O$	M11L	-0.007542	-4.732
$C_2H_5OH@H_2O$	MN12L	-0.007315	-4.590

We have studied the complex by using various functions with the choice of the basis set aug-cc-pVTZ. We have calculated the binding energy (B.E). The binding energy are in the range of -4.258 kcal/mol to -4.978 Kcal/mol for the ethanol and water complex. We infer that the complex, ethanol, and water form hydrogen bonds. Our results also satisfy the angle specifications given by IUPAC report [4]. In the Table(5.9), it is clear that the value of binding energy for ethanol and water complex in various functional shows strong hydrogen bonds [29].

Table 5.9: Binding energies of complex in different levels of approximation using basis set aug-cc-pVTZ

Complex	Level	$B.E.^a$ (Hartree)	$B.E.^b$ (kcal/mol)
$C_2H_5OH@H_2O$	B3LYP	-0.006795	-4.263
$C_2H_5OH@H_2O$	WB97XD	-0.007915	-4.966
$C_2H_5OH@H_2O$	M062X	-0.007934	-4.974
$C_2H_5OH@H_2O$	N12SX	-0.007940	-4.978
$C_2H_5OH@H_2O$	M11L	-0.007231	-4.533
$C_2H_5OH@H_2O$	MN12L	-0.006792	-4.258

5.4 Frequency Shift

An X-H bond lengthening and related red shift and increase in intensity in the IR spectrum are implied by a hydrogen bond between X-H and Y, where X is a more

electronegative atom or group than H and Y has a lone pair of electrons. These hydrogen bonds are known as "proper hydrogen bonds". However, a contraction of X-H bonds was observed, displaying so-called "improper hydrogen bonding"(blue-shifts with lower strength in the IR spectrum) [24]. The following factors influence the X-H bonds in all X-H atoms:

- In the presence of Y, the electron affinity of X results in a net increase in electron density at the X-H bond area and promotes an X-H bond contraction.
- An X-H bond elongation is caused by the well-known attractive interaction between the positive H and electron-rich Y [24].

Hobza and colleagues hypothesized that the incomplete electron transfer from the proton-accepting group (Y) to the chemical bonds in the proton-donating moiety other than X-H, strengthening and shortening the X-H bond, may be the cause of the incorrect blue-shifting hydrogen bond [25]. The following relationship can be used to determine the frequency shifts of X-H stretching modes:

$\triangle$V = V_1 - V = Negative, Red shift

$\triangle$V = V_1 - V = Positive, Blue shift

Where V_1 = Frequency of complex X-H stretching modes.

V= Frequency of free X-H stretching modes.

$\triangle$V = Change in frequency in X-H stretching modes.

Table (5.10) displays the frequency shift of the X-H stretching modes in the $C_2H_5OH...H_2O$ complex at various DFT approximation levels using the basis set selection of 6-311++G(d,p). We see that the change in frequency is minimum (-138.53 cm^{-1}) in the N12SX level of approximation for the $C_2H_5OH...H_2O$ complex and maximum (-85.99 cm^{-1}) in M062X level of approximation for the $C_2H_5OH...H_2O$ complex in Table (5.10). From our calculations, we obtain all frequencies are negative in different levels of approximation for the complex, which indicates the proper hydrogen bonding with X-H bond lengthening that is red-shift [30].

Table 5.10: Frequency shifts of X-H stretching modes in (cm^{-1}) using basis set 6-311++G(d,p), in different level of approximation .

Complex	Level	Complex X-H	Free X-H	Change	Shift
$C_2H_5OH@H_2O$	B3LYP	3721.40	3842.47	-121.07	Red
$C_2H_5OH@H_2O$	WB97XD	3798.07	3935.97	-137.9	Red
$C_2H_5OH@H_2O$	M062X	3830.22	3916.21	-85.99	Red
$C_2H_5OH@H_2O$	N12SX	3815.53	3954.06	-138.53	Red
$C_2H_5OH@H_2O$	M11L	3858.21	3949.71	-91.5	Red
$C_2H_5OH@H_2O$	MN12L	3860.09	3943.73	-83.64	Red

The frequency shift of X-H stretching modes in $C_2H_5OH...H_2O$ complex in DFT levels of approximation with the choice of basis set 6-311++G(2d,2p) is shown in Table(5.11). We see that the change in frequency is minimum (-144.17 cm^{-1}) in the N12SX level of approximation for the $C_2H_5OH...H_2O$ complex and maximum (-87.56 cm^{-1}) in MN12L level of approximation for the $C_2H_5OH...H_2O$ complex in Table (5.11). From our calculations, we obtain all frequencies are negative in different levels of approximation for the complex, which indicates the proper hydrogen bonding with X-H bond lengthening that is red-shift [30].

Table 5.11: Frequency shifts of X-H stretching modes in (cm^{-1}) using basis set 6-311++G(2d,2p), in different level of approximation .

Complex	Level	Complex X-H	Free X-H	Change	Shift
$C_2H_5OH@H_2O$	B3LYP	3721.55	3845.90	-124.35	Red
$C_2H_5OH@H_2O$	WB97XD	3796.23	3936.78	-140.55	Red
$C_2H_5OH@H_2O$	M062X	3811.95	3915.01	-103.06	Red
$C_2H_5OH@H_2O$	N12SX	3816.53	3960.70	-144.17	Red
$C_2H_5OH@H_2O$	M11L	3850.96	3947.57	-96.61	Red
$C_2H_5OH@H_2O$	MN12L	3875.33	3962.89	-87.56	Red

The frequency shift of X-H stretching modes in $C_2H_5OH...H_2O$ complex in DFT levels of approximation with the choice of basis set aug-cc-pVTZ is shown in Table(5.12). We see that the change in frequency is minimum (-151.75 cm^{-1}) in the

N12SX level of approximation for the $C_2H_5OH...H_2O$ complex and maximum (-91.76 cm^{-1}) in MN12L level of approximation for the $C_2H_5OH...H_2O$ complex in Table (5.12). From our calculations, we obtain all frequencies are negative in different levels of approximation for the complex, which indicates the proper hydrogen bonding with X-H bond lengthening that is red-shift [30].

Table 5.12: Frequency shifts of X-H stretching modes in (cm^{-1}) using basis sets aug-cc-pVTZ, in different level of approximation

Complex	Level	Complex X-H	Free X-H	Change	Shift
$C_2H_5OH@H_2O$	B3LYP	3693.13	3823.68	-130.55	Red
$C_2H_5OH@H_2O$	WB97XD	3768.83	3915.43	-146.60	Red
$C_2H_5OH@H_2O$	M062X	3790.47	3901.25	-110.78	Red
$C_2H_5OH@H_2O$	N12SX	3789.55	3941.3	-151.75	Red
$C_2H_5OH@H_2O$	M11L	3792.54	3888.1	-95.56	Red
$C_2H_5OH@H_2O$	MN12L	3791.56	3883.32	-91.76	Red

5.5 Zero Point Vibrational Energy

The Born-Oppenheimer approximation (BOA), which describes quantum chemistry, is typically accepted. As a result, the lowest point on the Born-Oppenheimer potential energy surface and zero point vibrational energy (ZPVE) are described as having different energies [31].

The zero-point vibrational energy of the complex has been obtained in the DFT levels of approximation with the choice of the basis sets 6-311++G(d,p), 6-311++G(2d,2p), and aug-cc-pVTZ in the present work. Zero point vibrational energy for the complex can be calculated by using the following relation.

ZPVE = ZPVE of the complex - ZPVE of the monomers

We have studied the zero point vibrational energy (ZPVE) of the complex in the DFT levels of approximations using basis sets 6-311+G(d,p) in a Table(5.13). The ZPVE is in the range of 1.54 kcal/mol to 1.85 kcal/mol for the ethanol and water complex. According to the IUPAC report [4], ZPVE does not have any significant effect on the stability of hydrogen bonds. It is seen in the Table(5.13), that the values of the

zero point vibrational energy (ZPVE) are almost peer in various functional for the ethanol and water complex.

Table 5.13: Zero Point Vibrational Energy (ZPVE), in kcal/mol using basis set 6-311++G(d,p), in different level of approximation .

Complex	Level	Zero point vibrational energy			
		Complex	Monomer1	Monomer2	ZPVE in kcal/mol
$C_2H_5OH@H_2O$	B3LYP	64.94	13.35	49.90	1.54
$C_2H_5OH@H_2O$	WB97XD	65.76	13.61	50.46	1.69
$C_2H_5OH@H_2O$	M062X	65.76	13.56	50.54	1.66
$C_2H_5OH@H_2O$	N12SX	66.03	13.66	50.65	1.72
$C_2H_5OH@H_2O$	M11L	65.43	13.78	49.80	1.85
$C_2H_5OH@H_2O$	MN12L	66.09	13.84	50.58	1.67

We have studied the zero point vibrational energy (ZPVE) of complex in the DFT levels of approximations using basis sets 6-311++G(2d,2p) in a Table(5.14). The ZPVE is in the range of 1.53 kcal/mol to 1.67 kcal/mol for the ethanol and water complex. According to the IUPAC report [4], ZPVE does not have any significant effect on the stability of hydrogen bonds. It is seen in the Table(5.14), that the values of the zero point vibrational energy (ZPVE) are almost equal in various functional for the ethanol and water complex.

Table 5.14: Zero Point Vibrational Energy (ZPVE), in kcal/mol using basis set 6-311++G(2d,2p), in different level of approximation .

Complex	Level	Zero point vibrational energy			
		Complex	Monomer1	Monomer2	ZPVE in kcal/mol
$C_2H_5OH@H_2O$	B3LYP	65.02	13.42	50.04	1.56
$C_2H_5OH@H_2O$	WB97XD	65.89	13.67	50.57	1.65
$C_2H_5OH@H_2O$	M062X	65.78	13.62	50.63	1.53
$C_2H_5OH@H_2O$	N12SX	66.11	13.72	50.75	1.64
$C_2H_5OH@H_2O$	M11L	65.23	13.81	49.75	1.67
$C_2H_5OH@H_2O$	MN12L	66.16	13.86	50.71	1.59

We have studied the zero point vibrational energy (ZPVE) of the complex in the DFT levels of approximation using basis sets aug-cc-pVTZ in the Table(5.15). The ZPVE is in the range of 1.4 kcal/mol to 2.15 kcal/mol for the ethanol and water complex. According to the IUPAC report [4], ZPVE does not have any significant effect on the stability of hydrogen bonds. It is seen in the Table(5.15), that the values of the zero point vibrational energy (ZPVE) are almost equal in various functional for the ethanol and water complex.

Table 5.15: Zero Point Vibrational Energy (ZPVE), in kcal/mol using basis set aug-cc-pVTZ, in different levels of approximation .

Complex	Level	Zero point vibrational energy			
		Complex	Monomer1	Monomer2	ZPVE in kcal/mol
$C_2H_5OH@H_2O$	B3LYP	64.71	13.33	49.91	1.47
$C_2H_5OH@H_2O$	WB97XD	65.64	13.58	50.47	1.54
$C_2H_5OH@H_2O$	M062X	65.44	13.52	50.52	1.40
$C_2H_5OH@H_2O$	N12SX	65.75	13.64	50.60	1.51
$C_2H_5OH@H_2O$	M11L	65.40	13.72	49.53	2.15
$C_2H_5OH@H_2O$	MN12L	65.78	13.78	50.54	1.46

5.6 Topological Analysis

We have studied bond critical points and their Laplacian of the electron density with the help of AIM (Atom in Molecules) with the basis sets; 6-311++G(d,p), 6-311++G(2d,2p), and aug-cc-pVTZ in the DFT levels of approximation. By the analysis of the topology of an electron, we have analyzed the presence of hydrogen bonding. According to the IUPAC report, analysis of the hydrogen-bonded system's electron density topology typically reveals a bond channel between H and Y as well as a (3,-1) bond critical point between H and Y [4]. The indication of a hydrogen bond has been proposed by Koch and Popelier as [32].

- $\rho = 0.002$ au to 0.034 au
- $\nabla^2\rho = 0.024$ au to 0.139 au. [where, au = atomic unit]

We have analyzed the type of bond by the analysis of the laplacian of the electron density at the bond critical point. If $\nabla^2\rho > 0$, then the bond is either hydrogen or vander waal or ionic bond whereas if $\nabla^2\rho < 0$, then the bond is covalent [33].
The optimized structure of the complex in the DFT levels of approximation using 6-31++G(d,p), 6-311++G(2d,2p), and aug-cc-pVTZ basis sets are shown in following figures, where HBCP represent the hydrogen bond critical point.

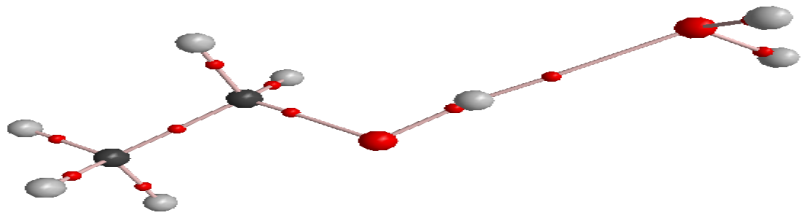

Figure 5.19: Structure of $C_2H_5OH...H_2O$ with bond critical points at the B3LYP level of approximation using 6-311++G(d,p) basis set. The bond critical points have been shown in between all the atoms that are bonded.

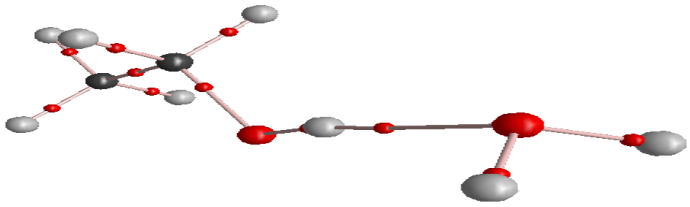

Figure 5.20: Structure of $C_2H_5OH...H_2O$ with bond critical points at the WB97XD level of approximation using 6-311++G(d,p) basis set. The bond critical points have been shown in between all the atoms that are bonded.

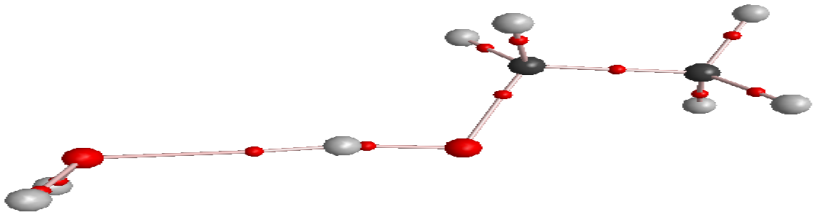

Figure 5.21: Structure of $C_2H_5OH...H_2O$ with bond critical points at the M062X level of approximation using 6-311++G(d,p) basis set. The bond critical points have been shown in between all the atoms that are bonded.

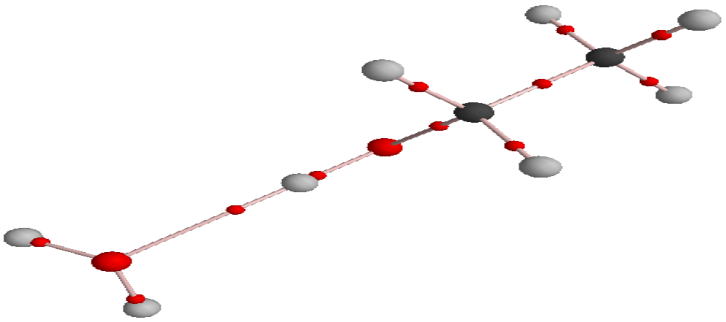

Figure 5.22: Structure of $C_2H_5OH...H_2O$ with bond critical points at the N12SX level of approximation using 6-311++G(d,p) basis set. The bond critical points have been shown in between all the atoms that are bonded.

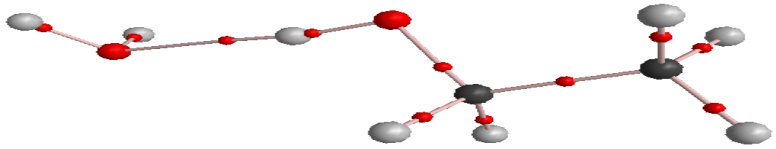

Figure 5.23: Structure of $C_2H_5OH...H_2O$ with bond critical points at the M11L level of approximation using 6-311++G(d,p) basis set. The bond critical points have been shown in between all the atoms that are bonded.

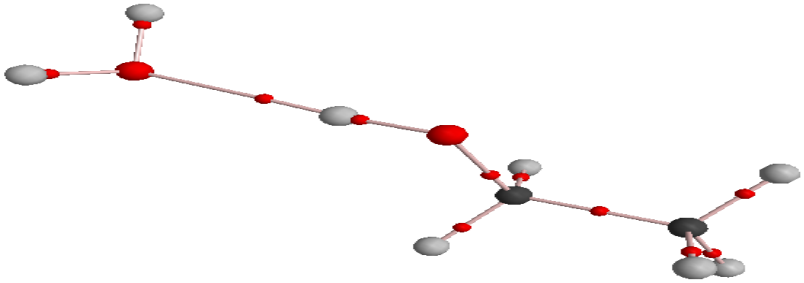

Figure 5.24: Structure of $C_2H_5OH...H_2O$ with bond critical points at the MN12L level of approximation using 6-311++G(d,p) basis set. The bond critical points have been shown in between all the atoms that are bonded.

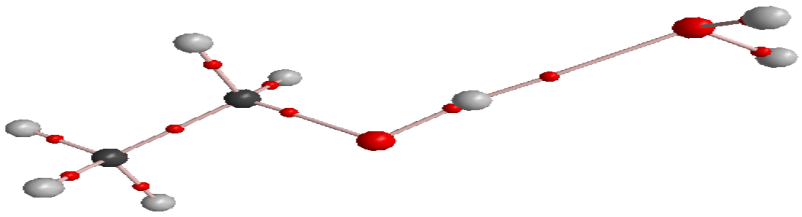

Figure 5.25: Structure of $C_2H_5OH...H_2O$ with bond critical points at the B3LYP level of approximation using 6-311++G(2d,2p) basis set. The bond critical points have been shown in between all the atoms that are bonded.

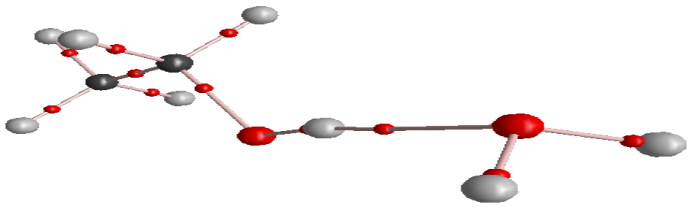

Figure 5.26: Structure of $C_2H_5OH...H_2O$ with bond critical points at the WB97XD level of approximation using 6-311++G(2d,2p) basis set. The bond critical points have been shown in between all the atoms that are bonded.

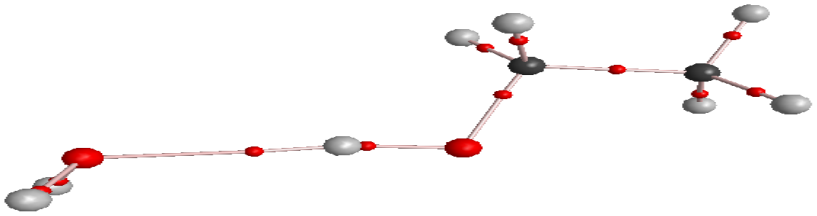

Figure 5.27: Structure of $C_2H_5OH...H_2O$ with bond critical points at the M062X level of approximation using 6-311++G(2d,2p) basis set. The bond critical points have been shown in between all the atoms that are bonded.

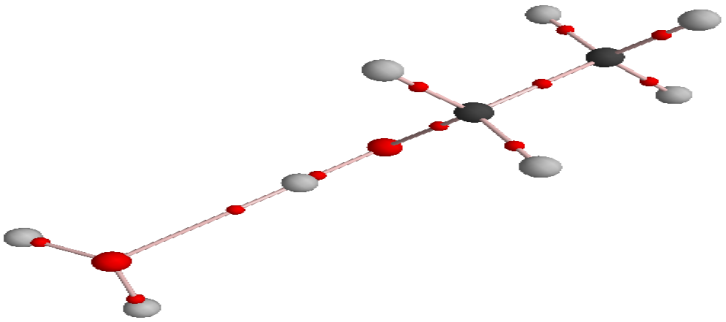

Figure 5.28: Structure of $C_2H_5OH...H_2O$ with bond critical points at the N12SX level of approximation using 6-311++G(2d,2p) basis set. The bond critical points have been shown in between all the atoms that are bonded.

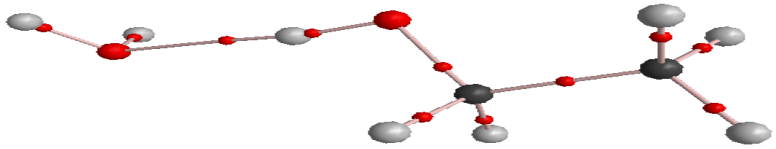

Figure 5.29: Structure of $C_2H_5OH...H_2O$ with bond critical points at the M11L level of approximation using 6-311++G(2d,2p) basis set. The bond critical points have been shown in between all the atoms that are bonded.

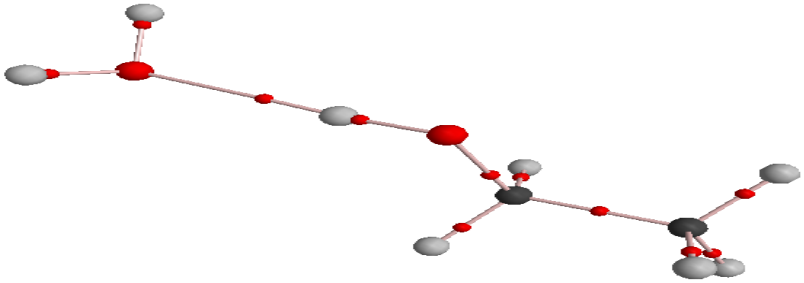

Figure 5.30: Structure of $C_2H_5OH...H_2O$ with bond critical points at the MN12L level of approximation using 6-311++G(2d,2p) basis set. The bond critical points have been shown in between all the atoms that are bonded.

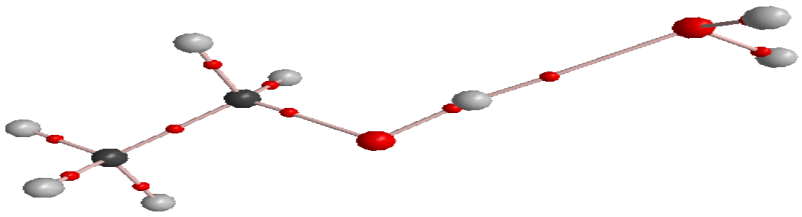

Figure 5.31: Structure of $C_2H_5OH...H_2O$ with bond critical points at the B3LYP level of approximation using aug-cc-pVTZ basis set. The bond critical points have been shown in between all the atoms that are bonded.

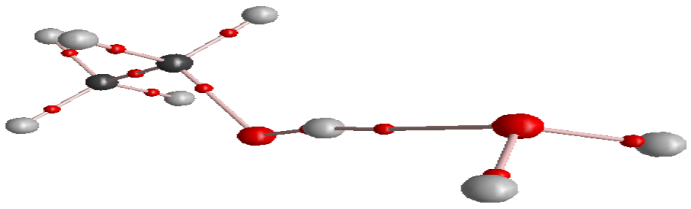

Figure 5.32: Structure of $C_2H_5OH...H_2O$ with bond critical points at the WB97XD level of approximation using aug-cc-pVTZ basis set. The bond critical points have been shown in between all the atoms that are bonded.

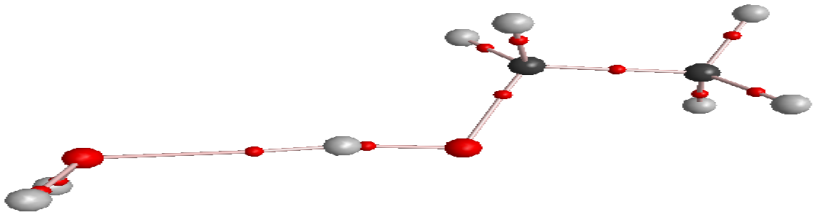

Figure 5.33: Structure of $C_2H_5OH...H_2O$ with bond critical points at the M062X level of approximation using aug-cc-pVTZ basis set. The bond critical points have been shown in between all the atoms that are bonded.

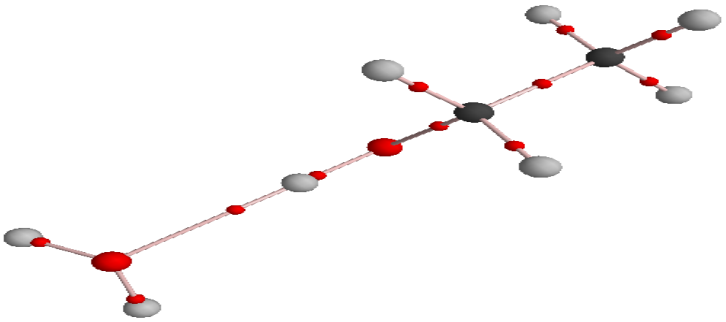

Figure 5.34: Structure of $C_2H_5OH...H_2O$ with bond critical points at the N12SX level of approximation using aug-cc-pVTZ basis set. The bond critical points have been shown in between all the atoms that are bonded.

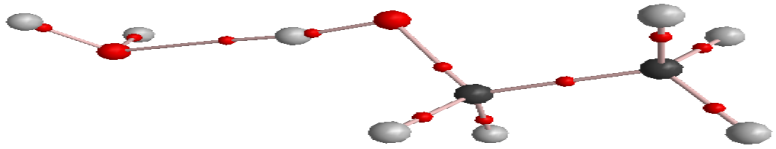

Figure 5.35: Structure of $C_2H_5OH...H_2O$ with bond critical points at the M11L level of approximation using aug-cc-pVTZ basis set. The bond critical points have been shown in between all the atoms that are bonded.

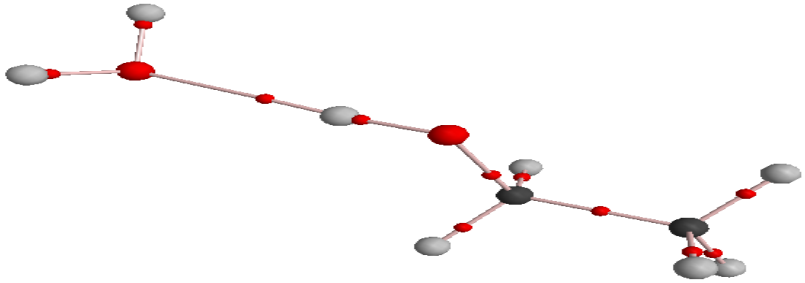

Figure 5.36: Structure of $C_2H_5OH...H_2O$ with bond critical points at the MN12L level of approximation using aug-cc-pVTZ basis set. The bond critical points have been shown in between all the atoms that are bonded.

The electron density (ρ) and laplacian of electron density ($\nabla^2\rho$) of the complex have been obtained in the different levels of approximation with the basis sets 6-311++G(d,p). In Table (5.16), the value of the ρ is in the range of 0.0199 au to 0.0261 au, which is slightly greater than the range given by Koch and Popelier [29] and the value of $\nabla^2\rho$ is in the range 0.0454 au to 0.0626 au, which also satisfies the condition for hydrogen bond formation. Admittedly, we have also compared our results with the observations of Oliveira and Vasconcellos, they carried out their

observation in the basis set aug-cc-pVDZ at the DFT(B3LYP) level of approximation; their results are comparable to ours [9].

Table 5.16: Topological analysis electron density and laplacian of electron density of complex in the different functional with the basis set 6-311++G(d,p).

Complex	Level	Geometry	
		ρ (au)	$\nabla^2\rho$ (au)
$C_2H_5OH@H_2O$	B3LYP	0.0240	0.0502
$C_2H_5OH@H_2O$	WB97XD	0.0261	0.0505
$C_2H_5OH@H_2O$	M062X	0.0242	0.0551
$C_2H_5OH@H_2O$	N12SX	0.0253	0.0626
$C_2H_5OH@H_2O$	M11L	0.0239	0.0566
$C_2H_5OH@H_2O$	MN12L	0.0199	0.0454

The electron density (ρ) and laplacian of electron density ($\nabla^2\rho$) of the complex have been obtained in the different levels of approximation with the basis sets 6-311++G(2d,2p). In Table (5.17), the value of the ρ is in the range of 0.0179 au to 0.0250 au, which is slightly greater than the range given by Koch and Popelier [29] and the value of $\nabla^2\rho$ is in the range 0.0450 au to 0.0620 au, which also satisfies the condition for hydrogen bond formation. Admittedly, we have also compared our results with the observations of Oliveira and Vasconcellos, they carried out their observation in the basis set aug-cc-pVDZ at the DFT(B3LYP) level of approximation; their results are comparable to ours [9].

Table 5.17: Topological analysis electron density and laplacian of electron density of complex in the different functional with the basis set 6-311++G(2d,2p).

Complex	Level	Geometry	
		$\rho(au)$	$\nabla^2\rho(au)$
$C_2H_5OH@H_2O$	B3LYP	0.0250	0.0602
$C_2H_5OH@H_2O$	WB97XD	0.0251	0.0505
$C_2H_5OH@H_2O$	M062X	0.0232	0.0551
$C_2H_5OH@H_2O$	N12SX	0.0213	0.0620
$C_2H_5OH@H_2O$	M11L	0.0229	0.0466
$C_2H_5OH@H_2O$	MN12L	0.0179	0.0450

The electron density (ρ) and laplacian of electron density ($\nabla^2\rho$) of the complex have been obtained in the different levels of approximation with the basis sets aug-cc-pVTZ. In Table (5.18), the value of the ρ is in the range of 0.0189 au to 0.0243 au, which is slightly greater than the range given by Koch and Popelier [29] and the value of $\nabla^2\rho$ is in the range 0.0354 au to 0.0605 au, which also satisfies the condition for hydrogen bond formation. Admittedly, we have also compared our results with the observations of Oliveira and Vasconcellos, they carried out their observation in the basis set aug-cc-PVDZ at the DFT(B3LYP) level of approximation; their results are comparable to ours [9].

Table 5.18: Topological analysis electron density and laplacian of electron density of complex in the different functional with the basis set aug-cc-pVTZ.

Complex	Level	Geometry	
		$\rho(au)$	$\nabla^2\rho(au)$
$C_2H_5OH@H_2O$	B3LYP	0.0230	0.0402
$C_2H_5OH@H_2O$	WB97XD	0.0231	0.0605
$C_2H_5OH@H_2O$	M062X	0.0232	0.0451
$C_2H_5OH@H_2O$	N12SX	0.0243	0.0626
$C_2H_5OH@H_2O$	M11L	0.0229	0.0466
$C_2H_5OH@H_2O$	MN12L	0.0189	0.0354

Chapter 6

Conclusion and Future Prospect

6.1 Conclusion

We have done the computational study of hydrogen bonded complex of ethanol and water using various functionals on the basis of density functional theory has been carried out using 6-311++G(d,p), 6-311++G(2d,2p), and aug-cc-pVTZ basis sets with the help of Gaussian-16 program. The computational calculations have been performed to study the binding energy, zero point vibrational energy, geometry parameters, frequency shift, and topological analysis. Our calculations are based on *ab initio* molecular orbital techniques.

We have studied bond distance and found to be in the range of 1.907Å to 2.103Å for DFT levels of approximation. From our calculation, the complex shows strong hydrogen bonding. The bond angle OH...X (X=H_2O) has a maximum value of 178.69° and minimum value of 172.73° for DFT levels of approximation by using different basis sets for complex ethanol and water.

We have calculated the binding energy of ethanol and water complex and found it to be in the range of -4.258 kcal/mol to -6.232 kcal/mol for DFT levels of approximation. We found that ethanol and water complex show the criteria of strong hydrogen bond and we have also studied zero-point vibrational energy. We have calculated the frequency shift of X-H stretching mode per cm and found it to be in the range of -85 cm^{-1} to -123 cm^{-1} for DFT levels of approximation. All the changes in frequency are negative that is red shift in ethanol and water complex in the case of O-H stretching mode. We have also calculated electron density and the laplacian of electron density

of the complex. We have obtained in the DFT levels of approximation with the basis sets 6-311++G(d,p), 6-311++G(2d,2p), and aug-cc-pVTZ, the value of $\nabla^2\rho$ is in the range of 0.0354 au to 0.0626 au and the value of the ρ is in the range of 0.0179 au to 0.0261 au. The ethanol and water complex satisfies the criteria for the values of ρ and $\nabla^2\rho$ for hydrogen bonds. In a nutshell, from the analysis of binding energy, zero-point vibrational energy, geometry parameters, frequency shift, and topological features of the electron density, we have seen the hydrogen bond in ethanol and water complex along with O-H interaction.

6.2 Future Prospect

We have studied different interactions in $C_2H_5OH...H_2O$ complexes. We can do the following study in the coming days:

- Similar study could be performed in higher basis sets.
- The other physical properties like dipole moment, polarizability, nuclear quadrupole, electric field gradients could also be calculated.
- Interaction in many other different complexes like organic compounds could be studied.

References

[1] C. Kittel, *Introduction to Solid State Physics*, Wiley- India (2009).

[2] L. Pauling, *The Nature of the Chemical Bond*, Cornell University Press, Ithaca, New York (1960).

[3] I. N. Levine, *Quantum chemistry*, PHI Learning, PHI Learning Private Limited, New Delhi (2012).

[4] E. Arunan, G. R. Desiraju, R. A. Klein, J. Sadlej, S. Scheiner, I. Alkorta, D. C. Clary, R. H. Crabtree, J. J. Dannenberg, P. Hobza, H. G. Kjaergaard, A. C. Legon, B. Mennucci, and D. J. Nesbitt, Pure Appl. Chem. **83**, 1619 (2011).

[5] Gaussian 16, Revision C.01, M. J. Frisch, G. W. Trucks, H. B. Schlegel, G. E. Scuseria, M. A. Robb, J. R. Cheeseman, J. A. Montgomery, Jr., T. Vreven, K. N. Kudin, J. C. Burant, J. M. Millam, S. S. Iyengar, J.Tomasi, V. Barone, B. Mennucci, M. Cossi, G. Scalmani, N. Rega, G.A. Petersson, H. Nakatsuji, M. Hada, M. Ehara, K. Toyota, R. Fukuda, J. Hasegawa, M. Ishida, T. Nakajima, Y. Honda, O. Kitao, H. Nakai, M. Klene, X. Li, J. E. Knox, H. P. Hratchian, J. B. Cross, V. Bakken, C. Adamo, J. Jaramillo, R. Gomperts, R. E. Stratmann, O. Yazyev, A.J. Austin, R. Cammi, C. Pomelli, J. W. Ochterski, P. Y. Ayala, K. Morokuma,G. A. Voth, P. Salvador, J. J. Dannenberg, V. G. ZakrzewskiS. Dapprich, A. D. Daniels, M. C. Strain, O. Farkas, D. K. Malick, A. D. Rabuck, K. Raghavachari, J. B. Foresman, J. V. Ortiz, Q. Cui, A. G.Baboul, S., J. Cioslowski, B.B. Stefanov, G. Liu, A. Liashenko,P. Piskorz, I. Komaromi, R. L. Martin, D. J. Fox, T. Keith, M. A. Al-Laham, C. Y. Peng, A. Nanayakkara, M. Challacombe, P. M. W. Gill,B. Johnson, W. Chen, M. W. Wong, C. Gonzalez, and J. A. Pople, Gaussian 03, Revision E.01, Gaussian Inc., Wallingford CT (2004).

[6] M. Ahmed, V. Namboodiri, A. K. Singh, J. A. Mondal, and S. K. Sarkar, J. Phys. Chem. B , **117**, 16479 (2013).

[7] A. D. Rabuck, G. E. Scuseria, J. Theor. Chem. Acc. **104**, 430 (2000).

[8] A. Dekhissi, L. Adamowicz, G. Maes, J. Phys. Chem. **104**, 2112 (2000).

[9] B. G. Oliveira and M. L. A. A. Vasconcellos, J. Mol. Struct. **774**, 83 (2006).

[10] S. Pal and T. K. Kundu, Int. Sch. Res. Notices., **2012** (2012).

[11] R. Parajuli and E. Arunan, J. Chem. Sci., **127**, 1035 (2015).

[12] H. Zhao, J. Chang , and L. Du, Comput. Theor. Chem., **1084**, 126 (2016).

[13] A. B. G C and R. Parajuli, J. Chem. Sci., **128**, 1191 (2016).

[14] B. K. Agrawal and H. Prakash, *Quantum Mechanics*, PHI Learning, New Delhi (2011).

[15] S. M. Blinder, J. Am. Phys., **33**, 431 (1965).

[16] A. Szabo and N. S. Ostlund, *Modern Quantum Chemistry: Introduction to Advanced Electronic Structure Theory, Dover Books on Chemistry*, Dover Publications (1996).

[17] N. M. Harrison, *An Introduction to Density Functional Theory*, London and CLRC (2004).

[18] C. Lee, W. Yang, and R. G. Parr, Phys. Review B. **37**, 787 (1988).

[19] P. Hohenberg and W. Kohn, Phys. Review. **136**, 864 (1964).

[20] J. B. Foresman and A. Frisch, *Exploring Chemistry with Electronic Structure Methods*, Gaussian, Inc., Pittsburgh (1996).

[21] L. K. Shrestha, Computational Study of the Properties of Cobalt Complexes $[Co(H_2O)_6]^{2+}$ and $[[Co(H_2O)_6](H_2O)_n]^{2+}$; n=1-4, M. Sc. (Physics) Dissertation,

Department of Physics, Amrit Campus, Tribhuvan University, Nepal (2019).

[22] R. Dennington, T. A. Keith, and J. M. Millam, Semichem Inc., Shawnee Mission, KS (2016).

[23] S. Puri, Computational Study of the Properties of Nickel Complexes $[Ni(H_2O)_6]^{2+}$ and $[[Ni(H_2O)_6](H_2O)_n]^{2+}$; n=1-4, M. Sc. (Physics) Dissertation, Department of Physics, Amrit Campus, Tribhuvan University, Nepal (2018).

[24] A. Szabo and N. S. Ostlund, *Modern Quantum Chemistry: Introduction to Advanced Electronic Structure Theory*, Dover Publications, New York (1996).

[25] J. B. Foresman and A. Frisch, *Exploring Chemistry with Electronic Structure Methods*, Gaussian, Inc., Pittsburgh (1995).

[26] P. Popelier, *Atoms in Molecules: An Introduction*, Pearson Education Limited (2000).

[27] E. R. Rosenberg, J. Phys. Chem. **116**, 10842 (2012).

[28] J. Chen, A. Mcallister, J. K. Lee and K. N. Houk, J. Org. Chem. **63**, 4611 (1998)

[29] G. A. Jeffrey, *An Introduction to Hydrogen Bonding*, Oxford University Press, Oxford (1997).

[30] J. Joseph and D. J. Eluvathingal, J. Am. Chem. Soc. **129**, 4620 (2007).

[31] K. K. Irikura, J. Phys. Chem. Ref. Data. **36**, 389 (2007).

[32] U. Koch and P. L. A. Popelier, J. Phys. Chem. **99**, 9747 (1995).

[33] C. F. Matta and R. J. Boyd, *An Introduction to the Quantum Theory of Atoms in Molecules*, WILEY- VCH Verlag GmbH and Co. KGaA, Wienheim (2007).